



Drought in the northern Bahamas from 3300 to 2500 years ago

Peter J. van Hengstum^{a, b, *}, Gerhard Maale^a, Jeffrey P. Donnelly^c, Nancy A. Albury^d, Bogdan P. Onac^e, Richard M. Sullivan^b, Tyler S. Winkler^b, Anne E. Tamalavage^b, Dana MacDonald^f

^a Department of Marine Science, Texas A&M University at Galveston, Galveston, TX, 77554, USA

^b Department of Oceanography, Texas A&M University, College Station, TX, 77843, USA

^c Coastal Systems Group, Woods Hole Oceanographic Institution, Woods Hole, MA, 02543, USA

^d National Museum of The Bahamas, PO Box EE-15082, Nassau, Bahamas

^e School of Geosciences, University of South Florida, Tampa, FL, 33620, USA

^f Department of Geosciences, University of Massachusetts-Amherst, Amherst, MA, USA, 01003

ARTICLE INFO

Article history:

Received 4 August 2017

Received in revised form

26 January 2018

Accepted 11 February 2018

ABSTRACT

Intensification and western displacement of the North Atlantic Subtropical High (NASH) is projected for this century, which can decrease Caribbean and southeastern American rainfall on seasonal and annual timescales. However, additional hydroclimate records are needed from the northern Caribbean to understand the long-term behavior of the NASH, and better forecast its future behavior. Here we present a multi-proxy sinkhole lake reconstruction from a carbonate island that is proximal to the NASH (Abaco Island, The Bahamas). The reconstruction indicates the northern Bahamas experienced a drought from ~3300 to ~2500 Cal yrs BP, which coincides with evidence from other hydroclimate and oceanographic records (e.g., Africa, Caribbean, and South America) for a synchronous southern displacement of the Intertropical Convergence Zone and North Atlantic Hadley Cell. The specific cause of the hydroclimate change in the northeastern Caribbean region from ~3300 to 2500 Cal yrs BP was probably coeval southern or western displacement of the NASH, which would have increased northeastern Caribbean exposure to subsiding air from higher altitudes.

© 2018 Elsevier Ltd. All rights reserved.

1. Introduction

Multiple proxy-based climate archives document significant hydroclimate variability in the tropical North Atlantic region during the Holocene. These include oxygen isotopic variability in speleothems (Mangini et al., 2007; Medina-Elizalde et al., 2010; Winter et al., 2011; Fensterer et al., 2013) and microfossils (Hodell et al., 1991, 2001), compound-specific stable isotope analysis (Lane et al., 2014), lake-level records (Holmes, 1998; Fritz et al., 2011; Burn et al., 2016), microfossils and sedimentology of inland saline ponds (Teeter and Quick, 1990; Teeter, 1995b; Dix et al., 1999), coastal lagoon sedimentology, mineralogy, and water level variability (Hodell et al., 2005a; Malaizé et al., 2011; Gregory et al., 2015; Peros et al., 2015), terrestrial landscape change through pollen analysis (Kjellmark, 1996; Leyden et al., 1998; Higuera-

Gundy et al., 1999; Kennedy et al., 2006; Lane et al., 2009; Slayton, 2010; Torrescano-Valle and Islebe, 2015), the Ti flux into the Cariaco Basin (Haug et al., 2001), among others. The Holocene-scale hydroclimate records that are available generally document increased precipitation during the Holocene Climatic Optimum when boreal summer occurred near perihelion (~8000–6000 years ago), which was followed by an overall drying pattern over the last ~5000 years (Hodell et al., 1991, 1995; Higuera-Gundy et al., 1999; Haug et al., 2001; Fensterer et al., 2013). Superimposed upon this long-term trend, the Caribbean has experienced multiple centennial-scale droughts whose regional expression can be variable.

Previous droughts on the Yucatan Peninsula in Mexico are well documented. In the current climate regime, there is a regional precipitation gradient from the dryer northern region (~900 mm yr⁻¹, ~21°N) to the wetter south (1700 mm yr⁻¹, ~17°N) (Hodell et al., 2005b). This gradient is driven by seasonal migration of the Intertropical Convergence Zone (ITCZ), where oceanic warming during the boreal summer displaces the Atlantic

* Corresponding author. Department of Marine Science, Texas A&M University at Galveston, Galveston, TX, 77554, USA.

E-mail address: vanhenp@tamug.edu (P.J. van Hengstum).

ITCZ and the tropical rain belt northward (Hastenrath, 1976, 1984; Hu et al., 2007). As such, droughts on the Yucatan Peninsula that are documented by lake level, pollen, and geochemical reconstructions at 4700–3600 Cal yrs BP, 3400–2500 Cal yrs BP, 2300–2100 Cal yrs BP, 1900–1700 Cal yrs BP, 1400–1300 Cal yrs BP, 730 Cal yrs BP, and 560 Cal yrs BP (Hodell et al., 2005a, 2005b; Torrescano-Valle and Islebe, 2015) are likely linked to meridional ITCZ displacements. However, the ITCZ is just one component of the Hadley Cell, so other areas in the tropical North Atlantic may experience different hydroclimate changes if Hadley circulation moves meridionally. As such, the spatial pattern, ocean-atmospheric forcing, and specific timing of Yucatan droughts on other Caribbean islands remains under investigation (Lane et al., 2014).

Compared with the Yucatan, knowledge of Holocene hydroclimate variability on Little Bahama Bank and Great Bahama Bank is still limited. A pollen-based reconstruction of landscape change on Andros Island (Church's Bluehole) indicates a dominance of salt- and drought tolerant shrubs typical in modern open and rocky sites (e.g., *Piscidia*-type, *Dodonaea*) from 3000 to 1500 years ago, which then shift to hardwoods and palms, and a final transition to the modern pine-dominated landscape by ~750 years ago (Kjellmark, 1996). In a pollen record from Emerald Pond (sinkhole) on Abaco, an increase in *Pinus* and a decrease in palm pollen during the last ~700 years was the most significant floral change over the last ~8000 years (Slayton, 2010), which was also noted by van Hengstum et al. (2016) in the pollen record from Blackwood Sinkhole. However, an increase in grass on the landscape from ~3200 to 2300 Cal yrs BP led Slayton (2010) to suggest this was a possible arid period in Abaco.

Here we present evidence for a megadrought from ~3300 to ~2500 years ago on the Little Bahama Bank (Fig. 1). This is documented through a multi-proxy (i.e., microfossils, geochemistry, sedimentology) sinkhole-lake level reconstruction using sediment cores from No Man's Land (NML) on Abaco Island (26.592°, -77.279°). The potential climatological forcing of this drought is also discussed, given that other Caribbean localities (e.g., Yucatan, Dominican Republic) have experienced synchronous aridity and Abaco Island is geographically far removed from precipitation caused directly by ITCZ convective activity (Fig. 1C and D). In contrast, the geographic position of the Little Bahama Bank makes it a key geographic locality to monitor the long-term behavior of the NASH (Fig. 1B).

2. Regional rainfall

Many large-scale ocean and atmospheric influences in the Pacific and Atlantic region impact Caribbean rainfall and evaporation (Hastenrath, 1976, 1984; Enfield and Alfaro, 1999; Gamble and Curtis, 2008), such as: the intensity and position of the North Atlantic Subtropical High (Davis et al., 1997; Giannini et al., 2000; Li et al., 2011, 2012a, 2012b), the position of the Caribbean Low Level Jet (Wang, 2007; Whyte et al., 2008; Martin and Schumacher, 2011a; Herrera et al., 2015), the Madden-Julian Oscillation (Martin and Schumacher, 2011b), seasonal migration of the ITCZ (Hastenrath, 1976), El Niño/Southern Oscillation (Nyberg et al., 2007; Jury, 2009), the North Atlantic Oscillation (Jury et al., 2007), hurricane activity, orographic effects (e.g., Cuba, Hispaniola) (Jury et al., 2007; Gamble and Curtis, 2008; Martin and Fahey, 2014), and sea surface temperatures in the North Atlantic warm pool (Wang et al., 2006).

On millennial timescales, meridional displacements of the ITCZ are thought to be important drivers of Caribbean rainfall. The ITCZ is a band of strong convective activity and precipitation caused by the convergence of the trade winds, which oscillates seasonally

between ~0° N and 13° N (see Fig. 2G in Hu et al., 2007). The zonally-averaged ITCZ position is suggested to have only moved <2° latitude during the Holocene based on time-sliced estimates of cross-equatorial atmospheric transport (McGee et al., 2014). However, there is evidence for Caribbean megadroughts across 18° N to 26° N during the Holocene. Therefore, regional ocean-atmospheric drivers of rainfall must be considered for understanding Caribbean hydroclimate variability on Holocene timescales.

In general, annual Caribbean rainfall is bimodal with dry season from November through April and a wet season from May to October. However, the wet season is interrupted by a rainfall decrease known as the 'Mid-Summer Drought' (Magaña et al., 1999; Jury et al., 2007; Gamble et al., 2008). It is thought that the Mid-Summer Drought is caused by seasonal intensification and south-western displacement of the NASH in the Caribbean region during boreal summer (Hastenrath, 1976, 1984; Gamble et al., 2008), in addition to potential amplifying effects from local vertical wind shear and atmospheric dust from Africa (Angeles et al., 2010). Gamble and Curtis (2008) presented a 5-part conceptual model to describe synoptic scale atmospheric drivers of annual and regional Caribbean rainfall patterns: (1) summertime expansion of the NASH, which decreases rainfall especially in the northeastern Caribbean, (2) large-scale subsidence concentrated at 70–75° W that decreases local precipitation [Zone 2 in Fig. 1B, see Fig. 4a Magaña and Caetano (2005)], (3) the Caribbean Low Level Jet that impacts the north coast of South America and the Lesser Antilles, (4) vertical wind shear, and (5) localized divergence of surface winds near Jamaica. Hastenrath (1976) observed that an early southward displacement and intensification of the NASH, stronger Trade Winds, and an equator-ward shift of the east Pacific ITCZ occurs during the winter preceding a particularly dry Caribbean summer. Likewise, the anomalously dry Caribbean decade from 1979 to 1989 CE has been attributed to intensification of the NASH (McLean et al., 2015).

Still further, the timing and amplitude of rainfall across the western tropical North Atlantic margin is also variable. In the northeastern-most Bahamian Archipelago (e.g., Little and Great Bahama Banks) and northwestern Cuba, annual rainfall exceeds 1300 mm yr⁻¹, as do the islands of Hispaniola, and those in the northern Lesser Antilles. However, Jury et al. (2007) documented that the southern Bahamian Archipelago, eastern Cuba, and Jamaica (Zone 2, Fig. 1B) receive only ~870 mm yr⁻¹ of rainfall. It is thought that reduced annual mean precipitation in the central Caribbean (Zone 2) relates to local subsidence caused by large-scale divergence as the anticyclone flow splits between an axis south of Cuba and one re-curving towards Florida (Jury et al., 2007; Gamble and Curtis, 2008). The Mid-Summer Drought occurs in July, August, and September in the northern Bahamas; but it happens in June, July, and August in the lower Bahamian Archipelago (Fig. 1E).

3. Study site

The Bahamian Archipelago is a group of carbonate islands and banks along the western tropical North Atlantic margin that began forming in the late Jurassic, and this region has since weathered into a mature karst landscape (Mullins and Lynts, 1977; Mylroie and Carew, 1995; Mylroie et al., 1995a, 1995b). Sinkholes and blueholes are an important source of paleoenvironmental and paleohydrological information because sediment and fossils deposited into these systems can remain protected from subsequent bioturbation or physical reworking (Crotty and Teeter, 1984; Kjellmark, 1996; Alvarez Zariqian et al., 2005; Steadman et al., 2007; van Hengstum et al., 2016).

No Man's Land on Great Abaco Island is one of the largest diameter inland lakes in the northern Bahamas (Fig. 2). In its

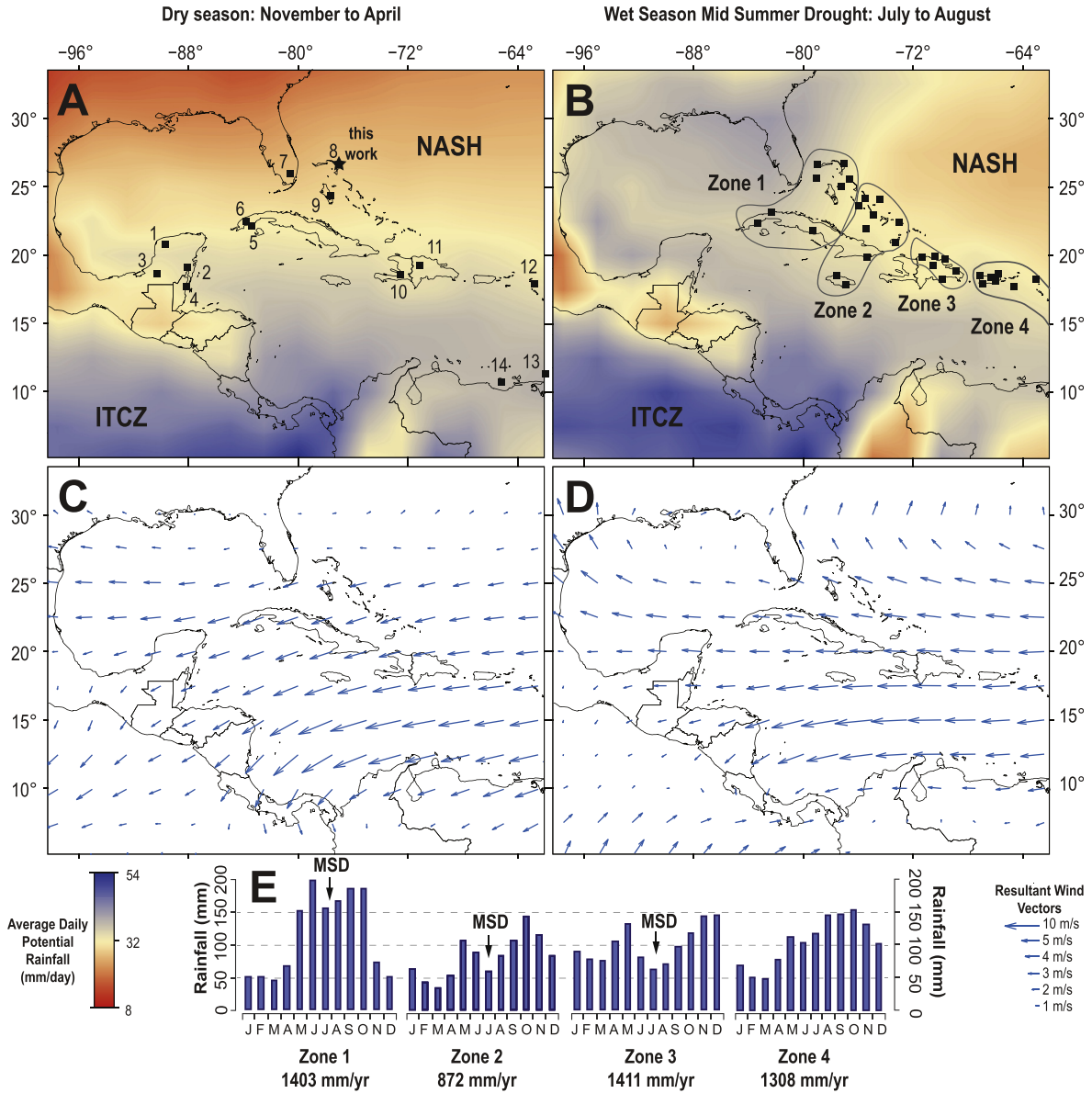


Fig. 1. Maximum daily potential rainfall (mm/day, 1948 to 2016 CE, Panel A and B) and resultant vectors of monthly mean wind (u/v) at 1000 mbar (m/s, 1986 to 2016 CE, Panel C and D) in the Caribbean region from the NCEP/NCAR Reanalysis Project, averaged over the November to April dry season, and the Mid-Summer drought from July and August on the Little Bahama Bank during the wet season. Panel A notes locations of other Caribbean climate records: (1) Aquada X'caamal, Mexico (Hodell et al., 2005a), (2) Lake Tzib, Mexico (Carrillo-Bastos et al., 2010), (3) Laguna Silvituc, Mexico (Torrescano-Valle and Islebe, 2015), (4) Turneffe Atoll, Belize (Wooller et al., 2009), (5) Playa Bailen and Punta de Cartas, Cuba (Gregory et al., 2015), (6) Dos Anas Cave, Cuba (Fensterer et al., 2013), (7) Northeast Shark River Slough, Florida (Glaser et al., 2012), (8) This work (No Man's Land), and Emerald Pond (Slayton, 2010), and Blackwood Sinkhole (van Hengstum et al., 2016), (9) Church's Bluehole, Andros (Kjellmark, 1996), (10) Lake Miragoane, Haiti (Hodell et al., 1991; Higuera-Gundy et al., 1999), (11) Valle de Bao, Dominican Republic (Kennedy et al., 2006), (12) Grand-Case Pond, Saint Martin (Malaizé et al., 2011), (13) Lake Antoine, Grenada (Fritz et al., 2011), (14) Cariaco Basin, Venezuela (Haug et al., 2001). The appearance of significant aridity above ~25°N is an artifact of long term averaging of the variable position of the western boundary of the NASH (Li et al., 2011). Panel B illustrates the four eastern Caribbean hydroclimate zones based on meteorological data from 1951 to 1981 CE from 35 stations (black squares, Jury et al., 2007), with Panel E describing the annual cycles for each zone. *Acronyms:* ITCZ: Intertropical Convergence Zone, NASH: North Atlantic Subtropical High, MSD: Mid-Summer Drought.

modern state, the site is shallow (3 m deep), brackish (20.6 psu), 170 m in diameter, and ~700 m from the coastline. Although definitive evidence is lacking (e.g., speleothems along peripheral cliff wall), the circularity of No Man's Land suggests that it is a destructional lake formed by karst processes, according to the model of carbonate lake formation of Park Bousch et al. (2014). Furthermore, destructive lakes can be subdivided into either lotic (open) systems that are well-connected into local groundwater systems (i.e., hydraulically-open), versus the lentic (closed) systems whose hydrologic conditions are independent from the local

coastal aquifer (i.e., hydraulically-closed)(Schmitter-Soto et al., 2002). No Man's Land should not be considered a closed basin due to the high porosity and permeability of the upper stratigraphy (i.e., Lucayan Aquifer) of the antecedent carbonate (Whitaker and Smart, 1997).

4. Methods

A seismic reflection survey was completed with an Edgetech 424 CHIRP to image the subbottom stratigraphy, generate a bathymetric

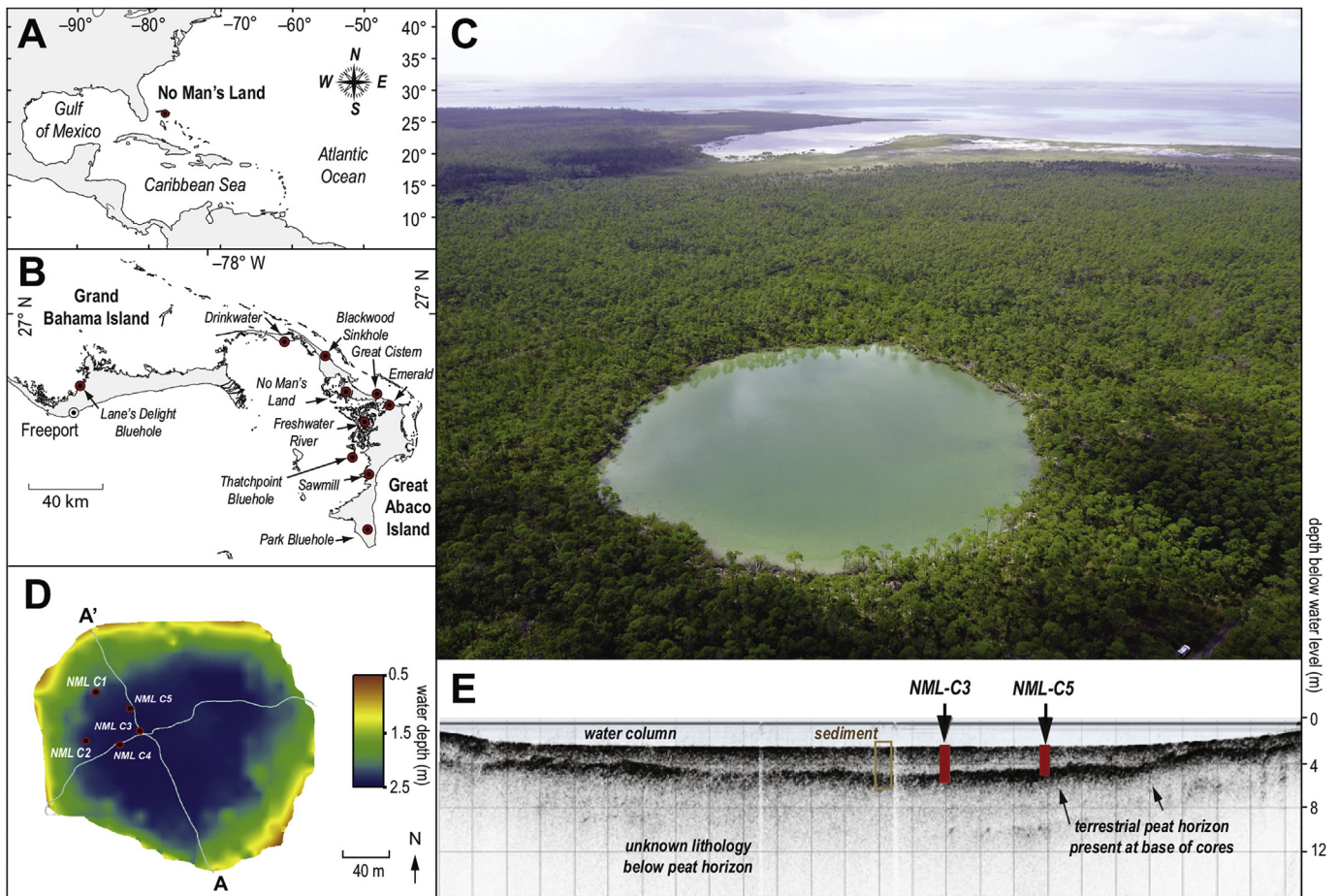


Fig. 2. (A) No Man's Land is located in the Northern Bahamas in the tropical North Atlantic Ocean. (B) Locations of prominent blueholes and sinkholes on the major islands of the Little Bahama Bank. (C) Aerial photograph of No Man's Land facing the west ('The Marls', and out to the Bight of Abaco). (D) Bathymetric map of No Man's and core locations. (E) Representative seismic reflection image along cross section A-A' from Panel B.

map, and identify targets for sediment coring (Fig. 2). Two-way travel time was converted to depth in meters using an assumed speed of sound in water of 1500 m/s. Five push cores were collected (70–120 cm in length) that all terminated on a terrestrial peat deposit, which correlates with a prominent acoustic reflector in the seismic reflection survey (Fig 2E, Fig. 3). After collection, sediment cores were split lengthwise in the laboratory, visually described following Schnurrenberger et al. (2003), photographed, X-radiographed to image sediment density, and subsequently stored at 4 °C until further analysis. Given the heterogeneity of the recovered sediment, the variability in the coarse fraction was analyzed using the Sieve-first Loss-on-Ignition (Sieve-first LOI) procedure (van Hengstum et al., 2016). This procedure is well suited to investigating the variability of the coarse sediment fraction in highly heterogeneous sediments from carbonate landscapes. Contiguous 1-cm sediment sub-samples with a standardized initial volume of 2.5 cm³ were first wet sieved over a 63- μ m mesh and dried for 12 h in an oven at 60 °C, and weighed to determine the original sediment mass. After they were dried and re-weighed, samples were ignited for 4.5 h at 550 °C in a muffle furnace to remove organic matter from the sediment samples to concentrate the remaining mineral residue. The variability in coarse sediment was then expressed as mass per unit volume ($D_{>63\ \mu\text{m}}\ \text{mg cm}^{-3}$). A classic LOI procedure was then performed on new sediment sub-samples at contiguous 1-cm intervals downcore to determine bulk organic matter variability as per standard methods (550 °C for 4.5 hrs)

(Dean Jr, 1974; Heiri et al., 2001).

The stable carbon isotopic value ($\delta^{13}\text{C}_{\text{org}}$) and C:N ratio of bulk organic matter from the recovered sapropel unit in core 4 and 5 ($n = 30$) was measured to investigate the possible salinity of the lake during its genesis (Rasmussen et al., 1990; Lamb et al., 2006; van Hengstum and Scott, 2011; van Hengstum et al., 2011). For comparative purposes, sediment samples ($n = 20$) were obtained from previously collected sediment cores from Mangrove Lake in Bermuda, which has been accumulating marine sapropel through the late Holocene (see Section 5.4). Carbonates were first digested from 1-cm sample sub-samples with a 10% HCl for 24 hrs, followed by residue desiccation at 80 °C and powdering. Measurements on samples from NML were then performed on a Costech ECS4010 Elemental Analyzer interfaced to a ThermoFisher Scientific Delta V Advantage Isotope Ratio Mass Spectrometer at the University of South Florida, with the samples from Mangrove Lake in Bermuda measured at the Baylor University Stable Isotope Laboratory by a Thermo-Electron Delta V Advantage Isotope Ratio Mass Spectrometer. Final results are expressed as ratios in the standard delta (δ) notation in per mil (‰) against Vienna PeeDee Belemnite (VPDB).

Cores 3, 4, and 5 were selected for detailed microfossil analysis to document changes in groundwater salinity on millennial timescales (Crotty, 1982; Teeter, 1989, 1995b; van Hengstum et al., 2008; van Hengstum et al., 2010; van Hengstum and Scott, 2012). No testate amoebae (thecamoebians) or agglutinated foraminifera

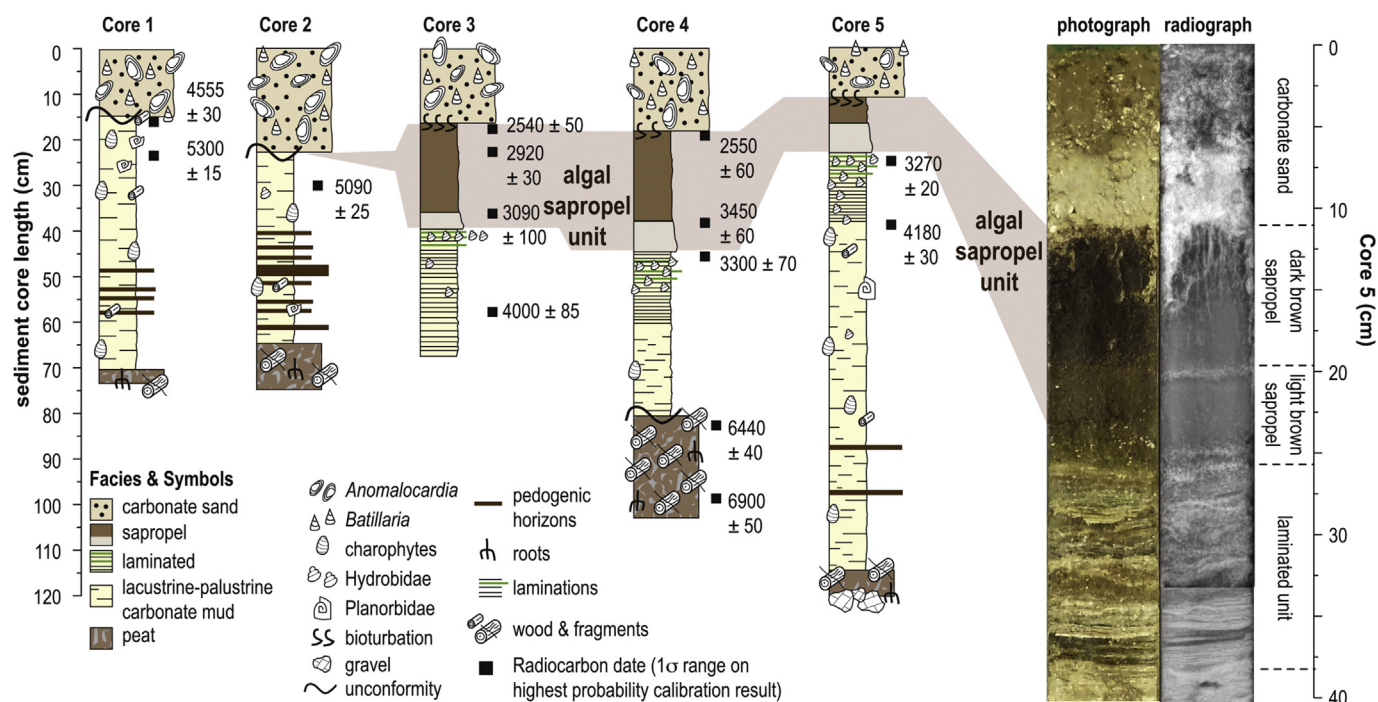


Fig. 3. Core logs for sediment cores from No Man's Land and representative photograph of upper section of core 4.

(e.g., *Trochammina inflata* or *Jadammina macrescens*) were observed during initial inspection of wet sediment residues that were concentrated on a 45- μ m mesh, but ostracodes were abundant. Ostracodes are crustaceans that are highly sensitive to salinity in their environment (Keyser, 1977), and their shell has a high preservation potential following death of the animal. During ostracode analysis, calcareous foraminifera were enumerated in cores 4 and 5, and charophyte gyrogonites (reported as individuals per cm^3) were counted from core 5. Charophytes are submerged macro-algae that are found in fresh to oligohaline waters, so their calcified fructifications (i.e., gyrogonites) are indicators of limnic to slightly brackish conditions (Soulié-Märsche, 2008; Soulié-Märsche and García, 2015).

Ostracodes were concentrated by wet-sieving a sediment subsample (1.25–2.5 cm^3) over a 63- μ m mesh to achieve census counts generally exceeding 120 valves per sample. The remaining coarse fraction was then dried overnight, and ostracode valves were picked from the dried residue and mounted onto standard micropaleontological slides. Taxonomy was verified with a Hitachi TM3000 desktop scanning electron microscope (Fig. 4), and followed available references (Furtos, 1933; Furtos, 1936; Swain, 1955; Van Morkhoven, 1963; Krutak, 1971; Keyser, 1975; 1977; Teeter, 1980, 1995a; Keyser and Schöning, 2000; Pérez et al., 2010a). Only 13 different taxonomic units of ostracodes were observed, thus, the estimated 2σ standard error on the ostracode relative abundance never exceeds 10%, with most standard error estimates in the range of 1–5% (Patterson and Fishbein, 1989). An original data matrix of 85 samples \times 13 ostracode observations was produced for Q-mode cluster analysis. Raw relative abundance data was first log transformed to emphasize broader ecological community patterns (Legandre and Legendre, 1998), and this data matrix was then subjected to unconstrained Q-mode cluster analysis using a Euclidian Distance coefficient to identify biofacies in the cores.

Wood fragments were submitted for radiocarbon dating to National Ocean Sciences Accelerator Mass Spectrometry when

available, but bulk organic material was dated when terrestrial plant macrofossils were absent at key stratigraphic horizons. The bulk organic matter dated was sapropel produced by aquatic algae. To help characterize the possible hardwater effect that was imparted on the bulk organic matter generated by algae living in groundwater, the conventional ^{14}C age of the twig sample from NML-C5 24–25 cm (3090 ± 20 conventional years ago) was subtracted from the bulk organic sample of NML-C4 46–47 cm (3730 ± 20 conventional years ago). It is assumed that these samples were deposited synchronously given the small size of the basin and their positioning below the same salient stratigraphic contact. This hardwater effect (640 ± 40 conventional years ago) was subtracted from the conventional ages obtained on other bulk organic matter samples. All radiocarbon ages were then calibrated into years before present (Cal yrs BP₁₉₅₀), where present refers to 1950 CE, using IntCal13 (Reimer et al., 2013). Only the highest probability 1σ calibration results are used in interpretations, but all calibration results are provided in Table 1. Detailed age models were not developed for the sediment cores because the most significant observation is the emplacement history for the primary stratigraphic units.

5. Results: stratigraphy, chronology, and microfossils

5.1. Terrestrial peat: prior to 6500 years ago

The basal sedimentary unit in the cores was a peat deposit (>70% organic matter, Figs. 3 and 5) that was accumulating until 6440 ± 40 Cal yrs BP, based on the limiting age on a twig from near the top contact with the carbonate mud unit in core 4. The deposit is a fragmental granular to woody peat because plant fragments ranged from 0.1 to >2 mm, and rootlets were not commonly observed (Schnurrenberger et al., 2003). No microfossils or invertebrate remains were observed in this unit.

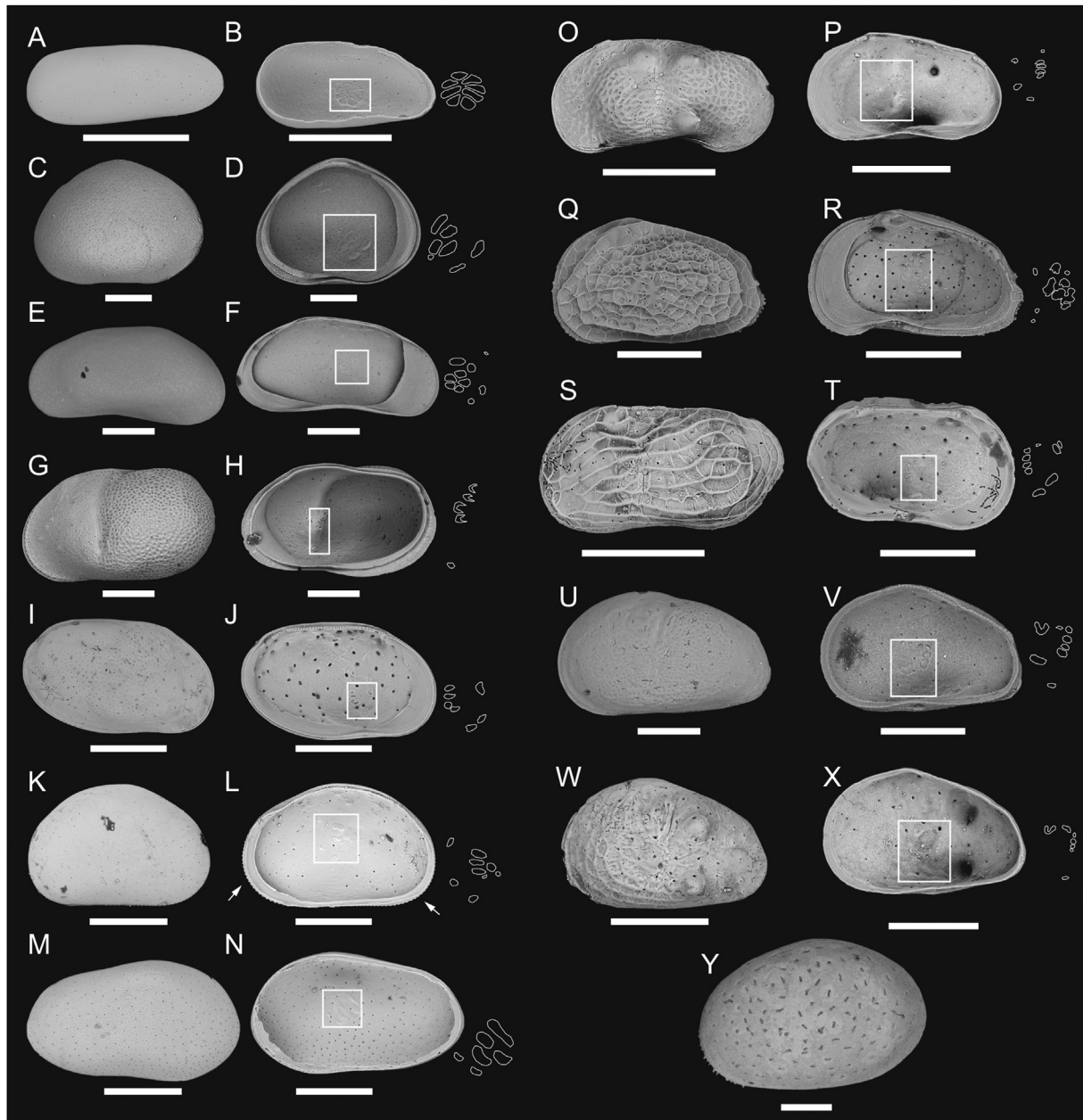


Fig. 4. Scanning electron micrographs of representative ostracodes and their dominant internal muscle scar pattern. (A, B) *Darwinula stevensoni* (Brady and Robertson, 1870); (C, D) *Cypridopsis vidua* (Müller, 1776), (E, F) *Candonina annae* (Mehes, 1914), (G, H) *Cytheridella ilosvayi* Daday, 1905, (I, J) *Loxoconcha matagordensis* Swain, 1955, (K, L) *Physocypria globulus* Furtos, 1933, arrows point to tuberculated margins on right valve, (M, N) Unknown sp., (O, P) *Limnocythere floridensis* Keyser, 1975, (Q, R) *Malzella floridana* (Benson and Coleman, 1963), (S, T) *Perissocytheridea bicelliforma* Swain, 1955, (U, V) *Cyprideis americana* (Sharpe, 1908), (W, X), *Cyprideis americana* var. nodes; (Y) *Haplocytheridella setipunctata* (Brady, 1869). Scale bar represents 250 μm .

5.2. Carbonate mud: 6500 to 4200 years ago

In all the cores, the basal peat deposit passes into a sequence of weakly-laminated carbonates that were deposited from ~6500 to ~4200 Cal yrs BP. The carbonate mud has a light grey to whitish hue, and contains gastropods tentatively placed within the families Planorbidae (c.f. *Heliosoma* sp. (Pilsbry, 1934) and Hydrobiidae (not identified). Organic content generally ranges from 4 to 15%, but was higher in occasional organic-rich horizons (e.g., core 1, 52–54 cm: 40%), and coarse sediment content was generally low ($D_{>63 \mu\text{m}}$ mg cm^{-3} : 0–25). Charophyte gyrogonites were present throughout the unit, but were most abundant towards the base of the facies (Fig. 6). The only foraminifera observed in this unit were *Helena*

davescottensis from 70 to 80 cm in core 4, which is a low salinity taxa previously described from palustrine-lacustrine marsh environments in Grand Bahamas (van Hengstum and Bernhard, 2016). No evidence of desiccation was observed (i.e., indurated or gypsum horizons).

Ostracodes were abundant, well preserved, and formed three biofacies in the carbonate mud unit (Fig. 6). The Freshwater Biofacies is from 95 to 112 cm in core 5, which is dominated by *Darwinula stevensoni* (mean 89.3%) and *Cypridopsis vidua* (mean 7.6%). The lack of a Freshwater Biofacies in core 4 indicates that sedimentation was not uniform during initial inundation of the basin, and that there is likely a depositional hiatus (i.e., disconformity) in cores 3 and 4 between the basal peat deposit and the carbonate

Table 1
Radiocarbon results.

Index No.	Accession number	Core	Core depth (cm)	Material dated	F ¹⁴ C	Conventional ¹⁴ C age	Hardwater Effect Removed (640 ± 40)	δ ¹³ C (‰)	1σ calendar ages in yrs. B ₁₉₅₀ (probability)	2σ calendar ages in yrs. B ₁₉₅₀ (probability)
1	OS-128591	C1	15 to 16	twig	0.6012 ± 0.0017	4090 ± 20		-26.5	4527–4584 (0.731) 4599–4609 (0.093) 4768 - 4782 (0.176)	4455 - 4457 (0.004) 4521–4644 (0.790) 4678 - 4692 (0.018) 4762 - 4800 (0.189)
2	OS-128592	C1	23 to 24	twig	0.5656 ± 0.0018	4580 ± 25		-28.09	5148 - 5151 (0.027) 5289–5320 (0.888) 5424 - 5433 (0.085)	5075 - 5106 (0.092) 5134 - 5163 (0.112) 5280–5323 (0.673) 5417 - 5442 (0.124) 5213 - 5296 (0.312)
3	OS-128595	C2	30	twig	0.5704 ± 0.0016	4510 ± 20		-25.77	5064–5112 (0.370) 5119 - 5149 (0.219) 5151 - 5184 (0.243) 5216 - 5221 (0.025) 5270 - 5289 (0.143)	5053–5190 (0.688)
4	OS-120797	C3	17 to 18	bulk organics	0.6749 ± 0.0015	3160 ± 20	2520 ± 60	-21.97	2494–2598 (0.544) 2610 - 2639 (0.151) 2681 - 2741 (0.305)	2380 - 2394 (0.016) 2402 - 2413 (0.010) 2424 - 2751 (0.974)
5	OS-128718	C3	23	leaf	0.7051 ± 0.0016	2810 ± 20		-27.1	2877–2929 (0.881) 2934 - 2943 (0.119)	2859–2959 (1.000)
6	OS-120796	C3	36 to 37	bulk organics	0.6401 ± 0.0018	3580 ± 25	2940 ± 65	-25.38	2995–3180 (0.977) 3200 - 3205 (0.023)	2888 - 2907 (0.013) 2922 - 3254 (0.957) 3294 - 3328 (0.029)
7	OS-120777	C3	57 to 58	stems	0.5844 ± 0.0015	4310 ± 20	3670 ± 60	-25.95	3920–4086 (1.000)	3840 - 4153 (1.000)
8	15OM/0483	C4	19.5 to 20	bulk organics	N/M	3150 ± 40	2510 ± 60	N/M	2492–2602 (0.554) 2607 - 2641 (0.167) 2678 - 2737 (0.279)	2379 - 2395 (0.019) 2400 - 2414 (0.018) 2421 - 2747 (0.963)
9	OS-120799	C4	38.5 to 39	bulk organics	0.6173 ± 0.0016	3880 ± 20	3240 ± 60	-24.83	3396–3509 (0.826) 3531 - 3556 (0.174)	3357 - 3608 (1.000) 3084 - 3087 (0.001)
10	OS-120798	C4	46 to 47	bulk organics	0.6287 ± 0.0015	3730 ± 20	3090 ± 60	-22.2	3228–3370 (1.000)	3156 - 3447 (0.999) 6319 - 6375 (0.107) 6386 - 6539 (0.893) 6790 - 6979 (1.000)
11	15P/0486	C4	83	bark	N/M	5660 ± 40		N/M	6405–6484 (1.000)	
12	OS-115026	C4	99	twig	0.4717 ± 0.0020	6040 ± 35		-28.42	6805 - 6812 (0.069) 6850–6942 (0.931)	
13	OS-113275	C5	24–25	twig	0.6803 ± 0.0016	3090 ± 20		-24.85	3254–3293 (0.611) 3328 - 3356 (0.389)	3241 - 3364 (1.000)
14	OS-115027	C5	39	twig	0.6205 ± 0.0019	3830 ± 25		-25.87	4155–4208 (0.592) 4219 - 4250 (0.331) 4273 - 4283 (0.078)	4103 - 4109 (0.006) 4148 - 4299 (0.924) 4327 - 4354 (0.045) 4369 - 4385 (0.018) 4392 - 4401 (0.007)

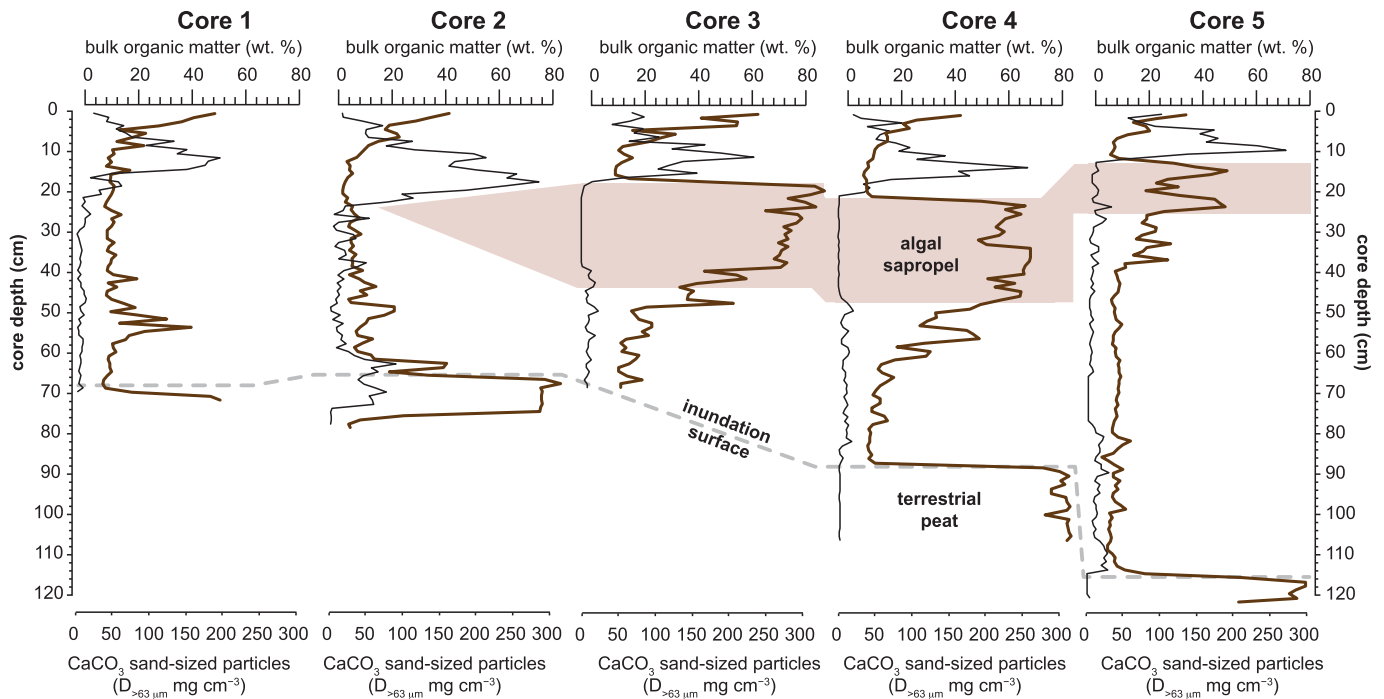


Fig. 5. Downcore bulk organic matter and textural variability. Brown line refers to bulk organic matter. (For interpretation of the references to colour in this figure legend, the reader is referred to the Web version of this article.)

mud. In core 5, the Freshwater Biofacies passes upsection into the Low Diversity Oligohaline Biofacies that is also present in cores 3 and 4. The Low Diversity Oligohaline Biofacies has a higher diversity than the Freshwater Biofacies, and is dominated by *Candona annae* (mean 25.8%), *Cypridopsis vidua* (mean 34.1%), *Darwinula stevensoni* (mean 19.3%), and *Limnocythere floridensis* (mean 19.2%). Finally, the uppermost biofacies in the carbonate mud unit is the High Diversity Oligohaline Biofacies, which is dominated by *Cypridopsis vidua* (87.2%) and *Candona annae* (10%), along with limited abundance of *Cytheridella ilyosvai* and an unidentified ostracode (Unknown sp.).

5.3. Laminated unit: 4200 to 3200 years ago

In the cores from the deeper part of the basin (cores 3, 4, and 5), the carbonate mud transitions upsection into 15–25 cm of laminated carbonate sediment that retained hues of green, purple, and brown. Deposition is temporally constrained by a radiocarbon dated twig in core 5 at 39 cm (4180 ± 30 Cal yrs BP), and at the upper contact with the algal sapropel unit in cores 5 and 4 (3270 ± 20 , 3300 ± 70 Cal yrs BP). Organic matter content increases from approximately 10% to >40%, and negligible vertical sediment mixing occurred based on the intact laminations throughout. The only ostracodes present were *Physocypria globula* (mean 68.3%) and *Cyprideis americana* (mean 31.5%), which comprise the Low Oxid Biofacies. *Physocypria globula* is a nektonic freshwater ostracode (Pérez et al., 2010b) that is diagnosed by the tuberculated margins of the right valve (Furtos, 1933). *Physocypria globula* dominates the assemblage at the onset of the Low Oxid Biofacies (e.g., 96% in core 4, 55.5 cm), but the topmost 1–2 samples of the biofacies (which were physically obtained from the algal sapropel unit; see Fig. 7) are dominated by *C. americana* (e.g., 100% at 39.5 cm in core 3) with highly friable valves.

5.4. Algal sapropel unit: ~3200 to 2500 years ago

Cores from slightly deeper water depths preserve an organic-rich algal sapropel unit (core 3: 17–40 cm, core 4: 20–48 cm, core 5: 12–26 cm). Onset of deposition is constrained by a radiocarbon date on a twig in core 5 to 3270 ± 30 Cal yrs BP, and dates at the upper contact with the carbonate sand unit in cores 3 and 4 of 2540 ± 50 and 2550 ± 60 Cal yrs BP, respectively. A leaf dated to 2920 ± 30 Cal yrs BP in core 3 at 23 cm is in stratigraphic succession with these minimum and maximum constraining ages (Fig. 3).

The sapropel could be divided into a lower light brown interval that was separated from a dark brown layer by a contact that is both visually distinct and present in the X-radiograph (core 3: 37 cm, core 4: 39 cm, core 5: 19 cm, Fig. 3). Overall, the algal sapropel had a mean $\delta^{13}\text{C}_{\text{org}}$ and C:N value of -23.8‰ and 15.3 ($n = 30$), respectively. However, organic matter in each separate layer of the algal sapropel unit had a slightly different geochemical signature. The stratigraphically lower, light brown layer had a mean $\delta^{13}\text{C}_{\text{org}}$ and C:N value of approximately -22‰ and 14, versus the stratigraphically higher dark brown layer that had values of approximately -25‰ and 14 (Fig. 8). Previously published $\delta^{13}\text{C}_{\text{org}}$ values indicate that organic matter generated by planktonic primary producers in marine versus freshwater aquatic settings are approximately -23‰ and -35‰ , respectively (France, 1995). For example, the $\delta^{13}\text{C}_{\text{org}}$ values are more depleted from a late Holocene freshwater sapropel from Carwash Cave System, Mexico (<4 psu) that accumulated over the last 6500 years ($n = 153$) (Fig. 8). The freshwater sapropel in Carwash Cave is derived from organic matter particles that are either transported into the cave from the terrestrial surface, or produced in the adjacent freshwater pond-like setting (van Hengstum et al., 2010). Furthermore, the $\delta^{13}\text{C}_{\text{org}}$ values and C:N ratio from the light brown NML sapropel are more enriched like the upper sapropel sediment from Mangrove Lake, Bermuda ($n = 20$, mean $\delta^{13}\text{C}_{\text{org}} = -18.6\text{‰}$, mean C:N = 10.5). Mangrove Lake is shallow (<2 m depth), with currently marine and

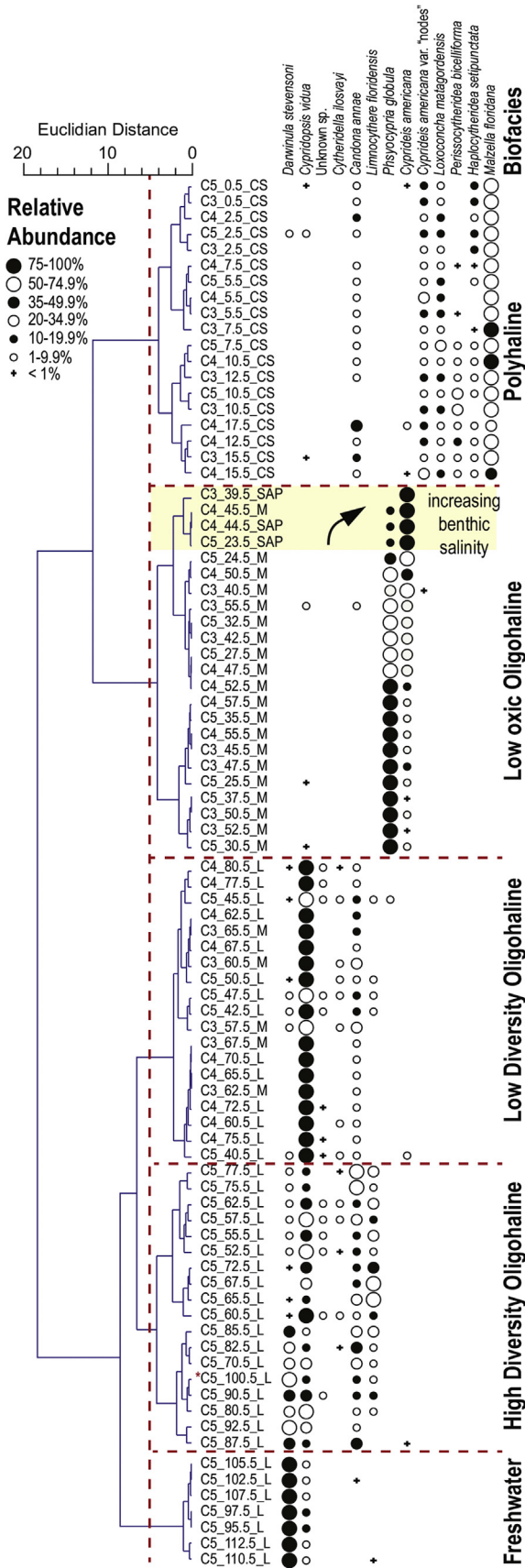


Fig. 6. Dendrogram produced from Q-mode cluster to identify biofacies in the ostracode data.

anoxic benthic conditions, and a similar marine sapropel has been accumulating in Mangrove Lake through the late Holocene (Hatcher et al., 1982, 1984; Watts and Hansen, 1986). These results indicate that salinity in NML during production and deposition of the lighter brown sapropel layer was slightly elevated in comparison to the darker brown layer, with a likely more marine salinity in the basin during deposition of the light brown sapropel unit.

The only microfossils preserved were the 1–2 samples dominated by *C. americana* at the base of the unit (as described above), which formed a visually distinct layer in the core. Taphonomically, the ostracode valves from the basal 1–2 cm of the algal sapropel unit were notably friable with evidence of dissolution on their shell surface (e.g., pitting). No other microfossils or carbonate particles were observed (e.g., testate amoebae, charophytes, or ostracodes), which is striking, given that microfossils are highly prolific in oxygenated Bahamian lakes, sinkholes, and coastal lagoons of any salinity regime (Dwyer and Teeter, 1991; Dix et al., 1999). At the top of the unit in the darker brown-hued layer were vertical burrows below the contact with the carbonate sand unit above.

5.5. Carbonate sand: ~2500 years ago until present

All core tops are characterized by a carbonate sand deposit (Fig. 3), and the contact between this unit and the underlying algal sapropel in cores 3 and 4 was 2540 ± 50 and 2550 ± 60 Cal yrs BP, respectively. The sand content decreases towards the top of each core because the modern sediment-water interface is covered by algae (Fig. 5). This indicates that the carbonate sand began deposition by 2500 Cal yrs BP. Both pelcypods and gastropods are abundant, which have been tentatively identified as *Anomalocardia* and *Batillaria*. The benthic foraminifera *Ammonia beccarii*, *Elphidium poeyanum*, and *Elphidium gunteri* were dominant (Fig. 7), with lesser abundances of *Triloculina oblonga*, and rare *Spirillina vivipara*. The carbonate sand unit contained the highest diversity ostracodes assemblage with the Polyhaline Biofaces (species richness of 10), and was dominated by *Malzella floridana* (mean 59.8%), *Cyprideis americana* var. “nodes” (mean 11%), *Loxoconcha matagordensis* (mean 11.5%), *Candona annae* (mean 7.7%), *Haplocytheridea setipunctata* (mean 4.6%), and *Perissocytheridea bicelliforma* (mean 4.5%). The presence of the ecophenotype *C. americana* var. “nodes” indicates this taxon is living near its lower limit of salinity tolerance because the development of nodes (tubercles, hollow protuberances) are a biological adaptation to lower salinity conditions (Meyer et al., 2017).

6. Discussion

6.1. Paleoenvironmental reconstruction of No Man’s land

The transition at ~6500 Cal yrs BP (core 4) from terrestrial peat deposition to carbonate mud with freshwater invertebrates (e.g., *Planorbis*) and charophytes indicates the onset of aquatic conditions in NML (Fig. 9). The ostracode assemblage is dominated by *Darwinula stevensoni* (Freshwater Biofacies), which is a widespread taxon that prefers salinities <2 psu (Keyser, 1977; Holmes, 1997; Pérez et al., 2010a). Along the periphery of the basin (cores 1 and 2), carbonate mud deposition is interspaced with brown organic-rich units containing plant fragments. The sediment and microfossils reflect palustrine-lacustrine environmental conditions in NML during the middle Holocene, which develop when carbonate-saturated groundwater floods a subaerial surface and promotes carbonate precipitation, but intermittent drying or localized vegetation can initiate some pedogenesis (e.g., cores 1 and 2) to create organic-rich horizons (Alonso-Zarza and Wright, 2010).

The onset of aquatic conditions in NML at ~6500 years ago was

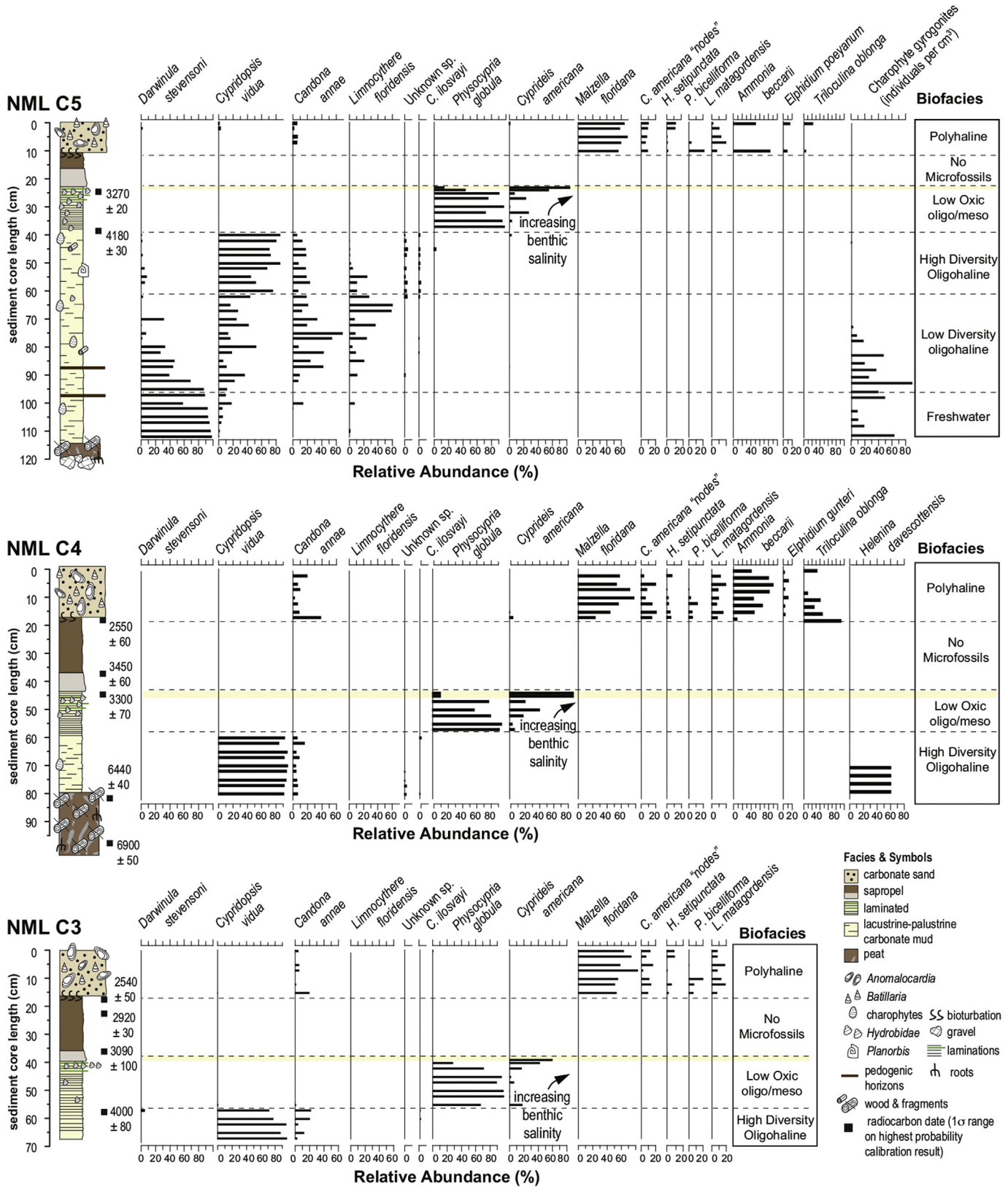


Fig. 7. Down core lithology, radiocarbon dates, and detailed microfossil changes and biofacies. Yellow highlighted intervals correspond to the increased abundance of *Cyprideis americana* (see Fig. 6), and abrupt increase in bottom water salinity. (For interpretation of the references to colour in this figure legend, the reader is referred to the Web version of this article.)

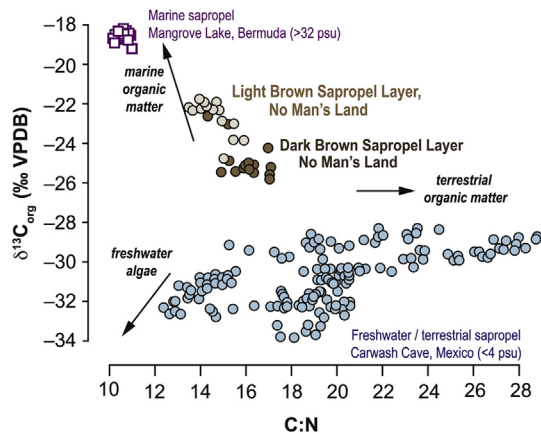


Fig. 8. Stable carbon isotopic value ($\delta^{13}\text{C}_{\text{org}}$) and C:N ratio of bulk organic matter from the algal sapropel unit in No Man's Land compared with those from a marine sapropel from Mangrove Lake in Bermuda ($n = 20, 32\text{--}35 \text{ psu}$) and a freshwater sapropel from Carwash Cave in Mexico (1.5 psu) (van Hengstum et al., 2010).

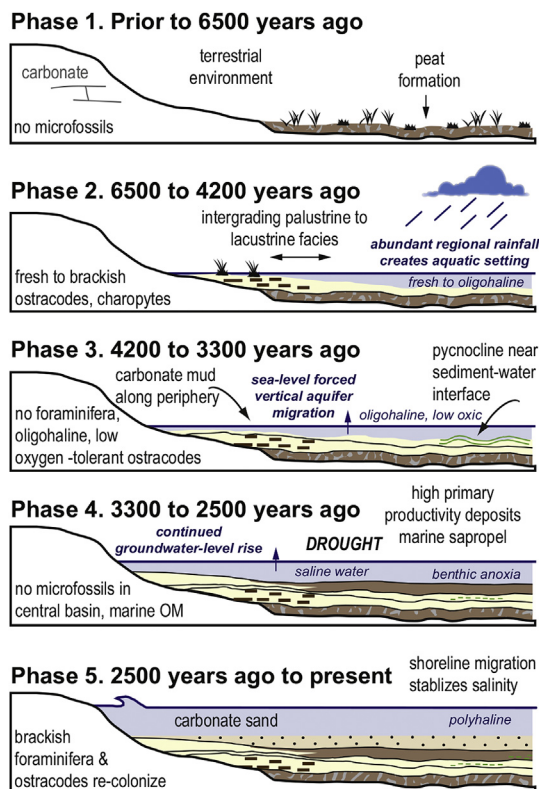


Fig. 9. Conceptual model describing paleoenvironmental changes in No Man's Land from 6500 years ago until present.

likely related to increased regional precipitation from a more northerly displaced ITCZ (Hodell et al., 1991, 1995; Fensterer et al., 2013). In general, the absolute elevation of the water table in porous eogenetic carbonate aquifers is dictated by local sea level. There is no stratigraphic evidence in NML for basin desiccation, suggesting that the shallow, freshwater aquatic environments were maintained after 6500 Cal yrs BP. A recent compilation of Bahamian sea-level indicators (Neumann and Land, 1975; Rasmussen and Neumann, 1988; Khan et al., 2017) that conform well to modeled estimates of relative sea-level rise (Milne and Peros, 2017, Fig. 10A) suggest that the bedrock bottom of NML may have been up to +1.5

m above sea level at ~6500 Cal yrs BP (Fig. 10A). Indeed, obtaining higher resolution local sea level indicators may help resolve this uncertainty. Nevertheless, aquatic freshwater environments would have been promoted by a more northerly ITCZ during the middle Holocene, which would have increased moisture delivery to the northern Bahamas, increased Ti flux to the Cariaco Basin (Haug et al., 2001), and depleted $\delta^{18}\text{O}$ values in both a Cuban speleothem (Fensterer et al., 2013) and lacustrine ostracodes from Haiti (Hodell et al., 1991). These proxies from elsewhere all indicate that ~7000 to ~5000 years ago was one of the wettest periods during the Holocene in the Caribbean. The additional supply of precipitation to the northern Bahamas likely promoted an increased flux of meteoric water and groundwater through NML, which likely initiated the mantling of carbonate sediment in the basin. At some point between ~5500 and 4500 Cal yrs BP, however, subsequent maintenance of the aquatic environments in NML would have been maintained by upward vertical migration of the coastal aquifer in response to Holocene sea-level rise.

Other ostracode biofacies in the carbonate mud unit (the High Diversity Oligohaline and Low Diversity Oligohaline Biofacies) most likely reflect habitat variability in NML between 6500 and 4200 years ago from (a) deepening of NML from concomitant Holocene sea-level and ground-water level rise, and (b) subtle climate-driven salinity variations in the oligohaline range (1–3.5 psu). The older, Lower Diversity Oligohaline Assemblage is dominated by *Cypridopsis vidua*, which is a cosmopolitan taxa that inhabits well-oxygenated lacustrine habitats across North America. It is also common in shallow, oligohaline waters in Florida (Keyser, 1977). In the Higher Diversity Oligohaline Assemblage, additional taxa appear that have a slightly higher salinity tolerance (e.g., *Cytheridella ilosvyi* in Core 5). Based on the ostracode fauna in the most expanded section of core 5, the increase in ostracode diversity through time (i.e., upsection) suggest that although the environment was primarily oligohaline, benthic conditions were likely fluctuating to slightly higher salinity regimes towards ~4200 Cal yrs BP.

It is worth noting that carbonate sedimentation does not appear uniform throughout the basin from 6500 Cal yrs BP until deposition of the carbonate sand unit at the top. There is likely a depositional hiatus between the peat and carbonate mud units in core 4, and the laminated and sapropel units are absent from cores 1 and 2. Given the bathymetric map and depth at which the hardground was encountered (Figs. 2 and 3), there appears to be a deepening of the hardground surface towards the center of the basin. As such, the deepest areas of the basin would have been inundated first by ponding water (core 5) relative to the basin margin (cores 1 and 2), and the variability in this surface likely lead to the hiatus in core 4. Despite the overall subtle relief on the hardground surface (<1 m), the recovered successions indicate that there was contemporary lateral facies transitions in NML. For example, pedogenic horizons were prevalent on the basin periphery (cores 1 and 2) than in deeper areas (cores 4 and 5, see Fig. 9). Overall, carbonate sedimentation in NML decreased as hydroclimate conditions began to shift towards aridity (discussed further below). First, carbonate sedimentation ceased along the periphery first to create a hiatus in cores 1 and 2 (no laminated mud unit), then in the deeper areas during deposition of sapropel. It is possible that enough fetch is available on NML to allow wave action to concentrate organic matter accumulation in the deepest areas of the base (cores 3, 4 and 5) during deposition of the sapropel. These results indicate just how sensitive sedimentation in inland tropical carbonate lakes is to both internal (e.g., basin geometry, bathymetry) and external factors (e.g., hydroclimate balance, local groundwater elevation and salinity changes).

At ~4200 Cal yrs BP, laminated carbonate sediment with

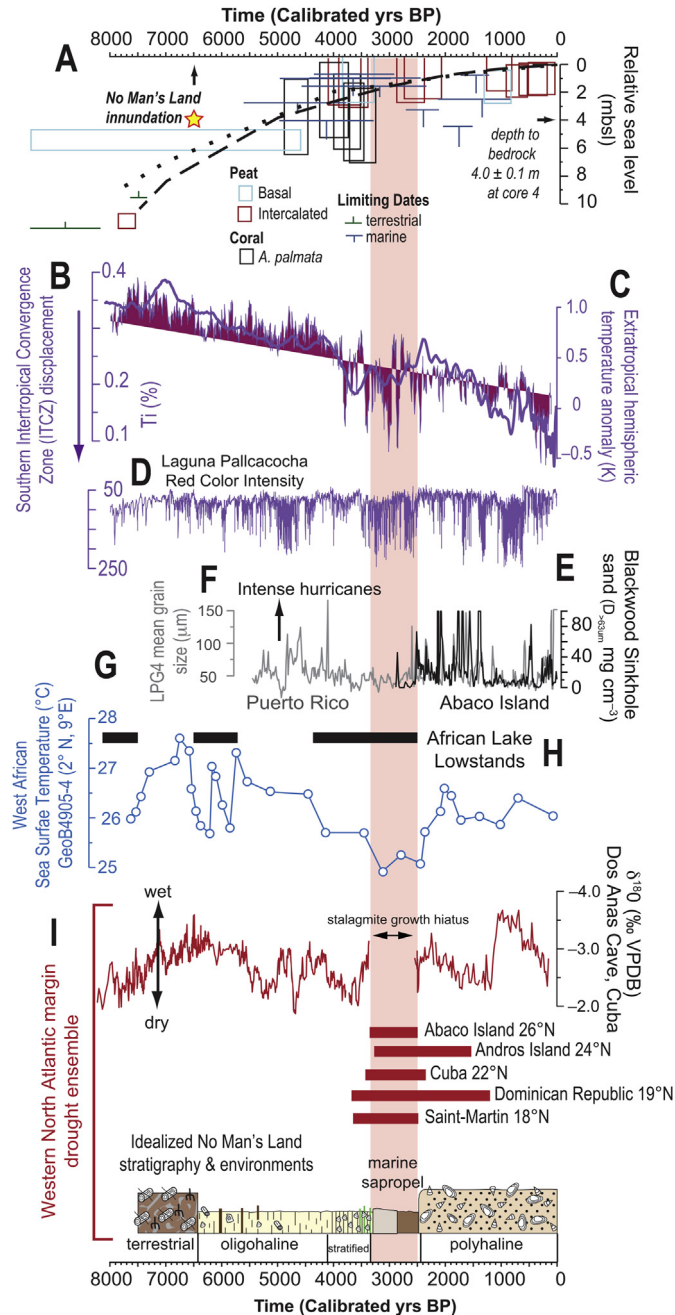


Fig. 10. Comparison of regional hydroclimate records with an idealized stratigraphic column from No Man's Land, Abaco Island, The Bahamas. (A) Regional sea-level framework after Khan et al. (2017), with additional older sea-level indicators from Abaco Island (Neumann and Land, 1975; Rasmussen et al., 1990), and ICE-5G model results with an upper mantle viscosity (UMV) = 5×10^{21} Pas and lower mantle viscosity (LMV) of 5×10^{22} Pas (dotted line) and EUST3 with an UMV = 2×10^{21} Pas and LMV = 5×10^{22} Pas (dashed line) (after Milne and Peros, 2013); evidence for southern displacement of the ITCZ based on (B) terrigenous runoff into the Cariaco Basin (light purple) and (C) inter-hemispheric extratropical temperature contrast (dark purple) (Haug et al., 2001; Schneider et al., 2014); (D) increased intense rainfall events around Laguna Pallcacocha, Ecuador (Moy et al., 2002); Intense hurricane activity on the western North Atlantic margin as recorded in Abaco (E) (van Hengstum et al., 2016) and Puerto Rico (F) (Donnelly and Woodruff, 2007); eastern equatorial Atlantic (off West Africa) sea surface temperature variability (G) (Waldeab et al., 2005) and evidence for African equatorial lake-level lowering (H) (Gasse, 2000), indicators of drought from ~3300 to 2500 on the Western North Atlantic (I), including speleothem growth hiatus in Dos Anas Cave in Cuba, (Fensterer et al., 2013), increased aridity-tolerant plants in Andros (Kjellmark, 1996) Abaco (Slayton, 2010), and the Dominican Republic (Kennedy et al., 2006), gypsum precipitation and anoxia in Cuban lagoons (Gregory et al., 2015), and coastal pond lowstand in Saint Martin, northern

gastropods began accumulating in deeper areas of NML. Microbialites in hypersaline lakes have deposited similar looking strata in the lower Bahamian islands (e.g., San Salvador) (Sipahioglu, 2010; Glunk et al., 2011), and freshwater microbialites are extremely rare (Garcia-Pichel et al., 2004; Gischler et al., 2008). The dominant ostracode in the laminated carbonate unit is the limnic *Physocypria globula* (>75%, Low Oxid Biofacies), but upsection in all cores the abundance of *P. globula* decreases and the relative abundance of *C. americana* increases to >90% (Fig. 6). Rather than microbialites, a more plausible explanation is that the laminated unit was deposited when a pycnocline was present near the sediment-water interface, and the benthos was seasonally, or intermittently, flooded by either a freshwater lens or anoxic saline groundwater. In Lago Petén Itzá (0.2 psu), *P. globula* was found tolerant of lower dissolved oxygen concentrations (to 2–4 mg/L), and to be an indicator of lake water below the thermocline in the hypolimnion (Pérez et al., 2010b). In Laguna de Yaxhá (25 m depth), Deevey et al. (1980) found *P. globula* (misidentified as *Cyprina petenesis*) to exhibit a planktic life mode, and tolerated deeper water with lower dissolved oxygen concentrations. Based on relative sea-level rise (Fig. 10A), concomitant vertical migration of the coastal aquifer and Holocene sea-level rise likely ensured that NML was permanently flooded by the upper section of the local coastal aquifer (i.e., meteoric lens) by 4200 Cal yrs BP, so the water column should have been ~1–2 m deep in NML (Figs. 9 and 10). The dominance of *P. globula* likely indicates a stratified freshwater column with lower dissolved oxygen concentrations in the hypolimnion during accumulation of the laminated unit. However, the upcore increase in *C. americana* likely indicates salinity was continually increasing at the sediment-water interface. Additional regional hydroclimate records will be required to resolve uncertainty as to whether this upcore microfossil trend is driven by Holocene sea-level rise (i.e., upward movement of freshwater lens), changing hydroclimate from an initial southern migration of the ITCZ at 4200 Cal yrs BP (see Figs. 9 and 10), or both. Nevertheless, the most significant observation is that *P. globula* indicates that NML was primarily limnic from ~4200 to 3300 Cal yrs BP, with potentially stratified oxygenation.

At ~3300 years ago, the stratigraphic and microfossil evidence collectively indicate that a shallow, stratified basin with a freshwater cap abruptly transitioned into an anoxic marine setting at 3200 Cal yrs BP. First, there is an abrupt increase in marine-tolerant ostracodes at the base of the sapropel unit in all cores whose shells are pitted and friable (90–100% samples of *C. americana* plot on the dendrogram with Low Oxid Biofacies in Fig. 6), which indicates a rapid increase in salinity and exposure to corrosive conditions. Second, the absence of benthic invertebrates in NML from 3300 to 2500 Cal yrs BP most likely indicates benthic anoxia, given the widespread distribution of freshwater to hypersaline-tolerant invertebrates (i.e., ostracodes, bivalves, gastropods) in the tropical North Atlantic lakes. Lastly, the $\delta^{13}\text{C}_{\text{org}}$ ratios indicate that phytoplankton living in marine conditions (lower light brown sapropel layer) initially produced the algal sapropel unit (Fig. 8). Perhaps some of the organic matter in the sapropel unit was generated during a seasonal brackish water-cap thereafter, but overall it was not produced by freshwater phytoplankton, as one would expect if a freshwater lens was present in NML. Based on local sea-level indicators, no abrupt change in sea-level occurred at 3300 Cal yrs BP, and NML should have been a stabilized aquatic environment by ~4200 Cal yrs BP (Fig. 9). Therefore, in order for the benthos in NML

to become flooded by anoxic saline groundwater for a multi-centennial time period, the local meteoric lens (freshwater lens) that was previously flooding NML must have abruptly contracted in response to decreased rainfall (discussed further below).

The final environmental transition in NML was the shift to the modern polyhaline (~20 psu) and well-oxygenated environment at ~2500 years ago. From a hydrogeological perspective, NML became flooded by a 'brackish water lens', which develops elsewhere in The Bahamas when meteoric water and saline groundwater are able to rapidly mix (Cant and Weech, 1986). At 2500 Cal yrs BP, NML was re-colonized by brackish gastropods (*Batillaria*), foraminifera (*Ammonia beccarii*, *Elphidium gunteri*, *Triloculina oblonga*), and ostracodes (*Malzella floridana*, *Loxoconcha matagordensis*), and infaunal bivalves (*Anomalocardia*) that bioturbated into the sapropel unit below. Continual shoreline migration associated with sea-level rise means that the land area (i.e., catchment) surrounding NML is no longer capable of generating and supporting an extensive freshwater lens, however, enough freshwater is available such that a local brackish water lens has become established.

6.2. Evidence and drivers of Caribbean drought and rainfall from 3300 to 2500 cal yrs BP

On Holocene timescales, relative sea-level rise causes the upward vertical migration of groundwater on carbonate platforms, which systematically causes landscape inundation and facies succession on exposed carbonate banktops. For example, the greatest depression on the antecedent Little Bahama Bank platform occurs in the Bight of Abaco, between Abaco Island and Grand Bahama Island. During its Holocene inundation, the local facies succession proceeded as follows: paleosol, limnic, brackish, hypersaline and finally marine (Rasmussen et al., 1990). In a similar depression on the Bermuda carbonate banktop (Port Royal Bay), Holocene facies progression included: freshwater peat, freshwater to oligohaline sapropel, followed by marine micrite deposition (Ashmore and Leatherman, 1984). In the case of NML, Holocene relative sea-level rise alone can not account for the observed facies succession (e.g., Section 6.1, onset of limnic conditions at ~6500 Cal Yrs BP, Fig. 10A).

Most importantly, the transition of NML from an oxic freshwater basin to an anoxic marine basin from 3300 to 2500 Cal yrs BP, followed by a reversion to a brackish basin is consistent with an abrupt change to a negative regional water balance. Both changes in land surface area and rainfall can influence the salinity at the water table on millennial timescales, assuming changes in topography and hydraulic conductivity of the coastal aquifer remain negligible (Cant and Weech, 1986). Intense hurricane activity can also be a significant factor to cause salinization of coastal carbonate aquifers (Holding and Allen, 2015), but 3300 to 2500 Cal yrs BP coincides with a less active period in terms of intense hurricane activity on the western tropical North Atlantic margin (Donnelly and Woodruff, 2007; van Hengstum et al., 2016). Smaller islands are associated with smaller freshwater lenses (Cant and Weech, 1986), but even Little Exuma Island has a freshwater lens (~1.6 km at widest point, 25.9 km² of land area, 0.89 km² of freshwater, less annual rainfall than Abaco: ~1000 mm yr⁻¹), whereas a brackish lens surrounds the area of NML (2.4 km wide, rainfall: ~1500 mm yr⁻¹). No abrupt sea-level change occurred during the last 3000 years to explain a concomitant reduction in land area and increased salinity at the water table (Fig. 10A). Indeed, inundation of tidal creeks and generation of wetlands to the north and south of NML would promote local groundwater salinization through increased aquifer evaporation, which likely explains the modern local brackish lens instead of a freshwater lens. However, this does not explain the loss of a freshwater lens at 3300 Cal yrs BP, then

subsequent regeneration of a brackish water lens in NML after 2500 Cal yrs BP. In the modern climate, brackish water lenses typically develop on Bahamian islands with rainfall below 900 mm yr⁻¹ (Cant and Weech, 1986). By extension, a decrease in regional rainfall, which was superimposed upon the long-term signal of relative sea-level rise, would explain the abrupt loss of a freshwater lens in NML from 3300 to 2500 Cal yrs BP.

3300 to 2500 Cal yrs BP is a known period of aridity in the tropical North Atlantic, but the drivers of aridity versus deluges at the island-scale remain an active area of research. This interval has been previously referred to as the 'Pan-Caribbean Dry Period' due to widespread evidence for aridity (Berman and Pearsall, 2000). It is likely that the Hadley Cell in the tropical North Atlantic region likely initiated a long-term, low-frequency southern oscillation at ~4000 Cal yrs BP, as evidenced by increased terrigenous runoff into the Cariaco Basin, decreased extratropical hemispheric temperature difference, and increased intense precipitation events in Laguna Pallcacocha in Ecuador (Fig. 10B, C, D). A shift of the ITCZ to the southern hemisphere is also supported by a cooling of sea surface temperatures (SSTs) in the western equatorial Atlantic from ~3700 to 2500 years ago at both 2°N (Waldeab et al., 2005) and 20°N (deMenocal et al., 2000). In the high latitudes, the most significant late Holocene reduction in North Atlantic Deep Water formation occurred at ~2800 Cal yrs BP (Oppo et al., 2003), which suggests both ocean and atmospheric changes at this time. Gasse (2000) reviewed increased aridity in equatorial Africa from ~4200 to 2200 years ago based on lowering of regional lake levels (e.g., Lake Bosumtwi, Bahr-el-Ghazal, Lake Abhé), and the most extreme changes in moisture balance occurred from 4200 to 4000 years ago. The cooling of the western equatorial Atlantic SSTs and changes in African terrestrial water balance are consistent with a southern displacement of the ITCZ from 4200 to 2500 years ago.

A southern displacement of the ITCZ from 4200 to 2500 Cal yrs BP and the rest of the northern Hadley Cell likely caused differential impacts on regional Caribbean hydroclimate, assuming late Holocene rainfall in the western tropical North Atlantic was like today and geographically variable (Fig. 1). Based on available records: (1) regions where modern rainfall is linked to seasonal ITCZ displacements appear to have rapidly responded to a lack of seasonal moisture delivery when the ITCZ moved southwards at ~4000 Cal yrs BP (e.g., Yucatan Peninsula, equatorial Africa), (2) regions where modern intensification or displacement of the NASH cause increased aridity seem to have become even more arid at ~3200 Cal yrs BP (Little Bahama Bank, Florida), and (3) regions where modern synchronous intensification of the NASH, easterlies, and Caribbean Low Level Jet deliver increased seasonal precipitation conversely become wetter during the Pan-Caribbean Dry Period (e.g., Grenada).

Building on the modern rainfall zones of Jury et al. (2007), precipitation in the northeastern Bahamas and Cuba is significantly linked to seasonal southwestern expansion of the NASH (Fig. 1). The collapse of the freshwater lens flooding NML from 3300 to 2500 years indicates that a change to the water balance in Abaco occurred. Previous pollen-reconstructions from Abaco (Blackwood Sinkhole and Emerald Pond) suggest that terrestrial vegetation (tropical hardwoods and palms) changed negligibly from 3200 to 2500 Cal yrs BP (Slayton, 2010; van Hengstum et al., 2016), other than a potential increase in grasses in the understory (Slayton, 2010). However, at least 4 species of bats on Abaco became extirpated after 3600 years ago (Soto-Centeno and Steadman, 2015), which may be related to the change in regional water balance that is documented by NML. On nearby Florida where rainfall is also linked to seasonality of the NASH, Glaser et al. (2012) documented a marked shift to drier conditions in the Everglades after 2800 Cal yrs BP. In northern Cuba, a speleothem collected from Dos Anas Cave

abruptly ceased growth from 3300 to 2500 Cal yrs (Fensterer et al., 2013). While speleothem growth hiatuses can also be driven entirely by stochastic processes, decreasing regional rainfall is also a significant environmental cause for disrupting speleothem growth. Elsewhere, shallow coastal lagoons in northern Cuba (Playa Bailen, Punta de Cartas) likely became anoxic and gypsum precipitated from approximately 3500 to 2500 years ago (Gregory et al., 2015), both of which could be caused by increased evaporation, decreased precipitation, and upward displacement of local saline groundwater.

Precipitation on the island of Hispaniola in the current climate is driven by both synoptic-scale atmospheric circulation and regional orographic effects from the Cordillera Central (Kennedy et al., 2006; Jury et al., 2007) (Martin and Fahey, 2014). Hydroclimate records from 3500 to 2500 Cal yrs BP on Hispaniola appear equivocal, but they do document an anti-phased hydroclimate shift between the northern versus southern regions that may elude to the combined effects of changing intensity of the trade winds and orographic effects. A pollen record from a high altitude bog (Valle de Boa) in the Cordillera Central indicates diminished moist-forest taxa and low water levels from ~3700 to 1200 Cal yrs BP (Kennedy et al., 2006). However, organic matter sedimentation did reinitiate at ~2500 Cal yrs BP, which suggests that the local watershed re-adjusted to some external forcing. Along the northern coast in the Dominican Republic, Laguna Saladilla documents a significant environmental change from ~3500 to 2500 years ago, but local geomorphologic effects introduce uncertainty on the specific magnitude and sign of water balance change (Caffrey et al., 2015). On the southside of the Hispaniola, a pollen record from Lake Miragoâne in Haiti documents the greatest relative abundance of pollen from mesic forest from ~7000 to 3200 years, after which a drying trend was initiated that likely caused extinction of local mammals, including bats, rodents, and a primate (Morgan and Woods, 1986; Higuera-Gundy et al., 1999). Stable oxygen isotopic ratios measured on benthic ostracodes (*Candona*) from Lake Miragoâne have a two-step enrichment from ~3200 to 2400 Cal yrs BP, then ~2400 to 1500 Cal yrs BP (Hodell et al., 1991). Similarly, there is a dominance of shrubs (e.g., *Piscidia*-type, *Dodonaea*) and minimal hardwoods or pinewoods on the low-lying Andros Island in the Bahamas from 3200 to 1500 years ago, which has been traditionally interpreted as indicating increasing aridity (Kjellmark, 1996). Still further, it remains uncertain how increased intense hurricane activity along the western tropical North Atlantic margin from 2500 to 1000 Cal yrs BP (Donnelly and Woodruff, 2007; van Hengstum et al., 2016) may be acting as a lurking variable impacting both terrestrial vegetation and lake hydrological records at this time.

Both lake hydrology and landscape flora indicate increased aridity on the Yucatan Peninsula (Mexico, Belize) from ~4000 to 2500 years ago and especially centered around ~3500 Cal yrs BP. In a 7900 year pollen record from Lake Silvituc, Mexico, a drought interval was inferred from 3400 to 2500 Cal yrs BP based on the decline of local tropical forest taxa *Moraceae*, *Brosimum alicastrum*, *Ficus*, among others (Torrescano-Valle and Islebe, 2015). The driest conditions of the last 8700 years in Lago Puerto Arturo was observed at ~3000 Cal yrs BP, based on enriched oxygen isotopic values on the gastropod *Pyrgophorus* (Wahl et al., 2014). Aguada X'caamal is a semi-closed sinkhole lake in the northern Yucatan whose lake water $\delta^{18}\text{O}$ ratio over the last 5000 years reflects both climate change and physical alteration of its hydrological budget (Hodell et al., 2005b). Notably, an abrupt shift to more ^{18}O -enriched subfossil ostracodes and gastropod shells from ~3200 to 2700 Cal yrs BP likely reflects decreased regional precipitation. In Lake Tzib, there is a shift to more enriched $\delta^{18}\text{O}$ values on the gastropod

Assiminea from 3500 to 2600 Cal yrs BP, with the appearance of disturbance taxa *Cecropia peltata*, *Croton*, and *Merremia* at 3500 Cal yrs BP (Carrillo-Bastos et al., 2010). On Turneffe Atoll, Belize, a vegetation shift from mangroves (*Rhizophora*) to *Chenopodiaceae*-*Amaranthaceae* and *Myrica* from 4100 to 2900 Cal yrs BP has been interpreted as environmental change driven by aridity (Wooller et al., 2009).

The impacts of decreased rainfall during this time also affected the subterranean component of the hydrologic cycle on the eastern Yucatan Peninsula in Mexico. Based on a 4-year hydrogeologic monitoring project (Coutino et al., 2017; Kovacs et al., 2017), increasing precipitation and salinity of the meteoric lens in the coastal aquifer covary because rainfall enhances mixing of the meteoric lens with the lower saline groundwater. As such, wetter climatic conditions can be expected to increase the net salinity of the coastal meteoric lens on millennial time-scales (Kovacs et al., 2017). Using sediment cores collected from an underwater cave flooded by the coastal aquifer near Tulum on the Yucatan (Carwash Cave), van Hengstum et al. (2010) used microfossils to document a low-frequency stepwise-decrease in the salinity of the meteoric lens over the last 5000 years, most likely in response to southern migration of the ITCZ (Hodell et al., 1991; Haug et al., 2001). Indeed, the sedimentation rate is variable in Carwash Cave through time, but the microfossils documented three salinity phases: (i) High Oligohaline (>3.5 psu): 6500–4300 Cal yrs BP, (ii) Medium Oligohaline (2–3.5 psu): 4200 to ~2700 Cal yrs BP, and (iii) Low Oligohaline (1.5 psu): 2700 Cal yrs BP to present. The stepwise and low-frequency salinity decreases in Carwash Cave from 4200 to 2700 Cal yrs BP do partially overlap with the Pan-Caribbean Drought (3200–2600 Cal yrs BP). It is possible that the proximity of Carwash Cave to the ITCZ may be responsible for the earlier onset for the effects of decreased rainfall, and its subsequent impact on decreased aquifer salinity (Kovacs et al., 2017), similar to equatorial African locales.

In contrast to higher Caribbean latitudes, the southern Lesser Antilles experienced increasing rainfall from 3300 to 2500 Cal yrs BP. In Lake Antoinne in Grenada (Fig. 1A), increasing abundance of the diatom *Pseudostaurosirella brevistriata* indicates the lake deepened from increased rainfall from 3200 to 2600 years ago (Fritz et al., 2011). Despite observations of drought elsewhere in the tropical North Atlantic at this time, the local response in the Lesser Antilles can be reconciled with both intensification and southern displacement of the NASH from a southern Hadley Cell displacement. In the modern climate, seasonal precipitation in the Lesser Antilles is more unimodal in comparison to elsewhere in the tropical North Atlantic, with a poorly developed Mid-Summer Drought during the wet season (Jury et al., 2007). Coincident with the seasonal intensification of the NASH causing the Mid-Summer drought in Zone 1 (Fig. 1), intensification the Caribbean Low Level Jet (CLLJ) in the lower tropical latitudes causes a seasonal precipitation maximum. The CLLJ is a localized amplification of easterly zonal winds at 925 hPa that positively co-vary with intensification of the NASH, and the CLLJ plays a critical role transporting moisture from the tropical North Atlantic Ocean into the Caribbean Sea (Wang, 2007; Martin and Schumacher, 2011a). Indeed, intensified easterly trade winds can be inferred from an increase in the upwelling indicator *Globigerina bulloides* in the Cariaco Basin from 3300 to 2500 Cal yrs BP (Peterson et al., 1991). Based on modern relationships between the NASH and CLLJ, one would expect that rainfall in the lower Lesser Antilles and northern Bahamas may be anti-phased over the last several millennia, but additional hydroclimate records are needed to test this hypothesis.

7. Conclusions

- A sinkhole–lake level reconstruction from Abaco Island on the Little Bahama Bank documents an abrupt shift from a freshwater environment that is low oxic, to a marine environment with benthic anoxia from 3300 to 2500 Cal yrs BP.
- Given constraints from low rates of relative sea-level rise during the late Holocene, the change in bottom water conditions is most likely linked to contraction of the local freshwater lens from a change in local water balance (decreased precipitation or increased evaporation).
- This suggests that the Little Bahama Bank experienced a drought from 3300 to 2500 years ago, similar to other Caribbean islands. However, it remains uncertain how the seasonality of precipitation changed.
- When considering the geographic location of Abaco Island and regional drivers of Caribbean rainfall, this change in local water balance from 3300 to 2500 years ago on the Little Bahama Bank is likely linked to decreased moisture delivery to Abaco from southward or westward expansion of the NASH synchronous with southern ITCZ displacement.
- These results further contribute to our growing knowledge on the geographic and temporal variability of Holocene hydroclimate extremes in the tropical North Atlantic, and provide several testable hypotheses for further numerical and climate modeling and paleoclimate reconstructions.

Acknowledgements

Fieldwork in The Bahamas was supported by the Friends of the Environment and permits issued by The Bahamas National Trust and The Bahamas Environment, Science and Technology (BEST) Commission. This research was supported by NSF grants OCE-1356509 and EAR-1703087 (PvH) and OCE-1356708 and EAR-1702946 (JPD), and the John W. Hess Student Research Grant from the Gerontological Society of America (to GM, EAR-1354519). Additional field and technical support was provided by Shawna Little, Victoria Keeton, Brian Albury, and Karl Kaiser. We benefited from discussions with Jason Gulley, and we thank Davin Wallace for providing the sediment samples from Mangrove Lake for geochemical analysis. The final version of this manuscript was improved through thoughtful evaluation by an anonymous reviewer and Sally Horn.

Appendix A. Supplementary data

Supplementary data related to this article can be found at <https://doi.org/10.1016/j.quascirev.2018.02.014>.

References

- Alonso-Zarza, A.M., Wright, V.P., 2010. Palustrine carbonates. In: Alonso-Zarza, A.M., Tanner, L.H. (Eds.), *Carbonates in Continental Settings*. Elsevier, Amsterdam, pp. 103–131.
- Alvarez Zariqian, C.A., Swart, P.K., Gifford, J.A., Blackwelder, P.L., 2005. Holocene paleohydrology of Little Salt Spring, Florida, based on ostracod assemblages and stable isotopes. *Palaeogeogr. Palaeoclimatol. Palaeoecol.* 225, 134–156.
- Angeles, M.E., González, J.E., Ramírez-Beltrán, N.D., Tepley, C.A., Comarazamy, D.E., 2010. Origins of the Caribbean rainfall bimodal behaviour. *Journal of Geophysical Research-Atmospheres* 115, D11106.
- Ashmore, S., Leatherman, S.P., 1984. Holocene sedimentation in Port Royal Bay, Bermuda. *Mar. Geol.* 56, 289–298.
- Benson, R.H., Coleman, G.L., 1963. Recent Marine Ostracodes from the Eastern Gulf of Mexico. The University of Kansas Paleontological Contributions Arthropoda, pp. 1–52.
- Berman, M.J., Pearsall, D.M., 2000. Plants, people, and culture in the prehistoric Central Bahamas: a view from the three dog site, an early lucayan settlement on san salvador island, Bahamas. *Lat. Am. Antiq.* 11, 219–239.
- Brady, G.S., 1869. In: De Folin, L., Périer, L. (Eds.), *Description of Ostracoda (from Hong Kong, Nouvelle Providence, Saint Vincent, Golfe de Gascogne, Colon Aspinwall, Port-au-Prince)*. Le Fonds de la Mer, Paris, pp. 122–127.
- Brady, G.S., Robertson, D., 1870. The ostracoda and foraminifera of tidal rivers. *Ann. Mag. Nat. Hist.* 6, 1–33.
- Burn, M.J., Holmes, J., Kennedy, L.M., Bain, A., Marshall, J.D., Perdikaris, S., 2016. A sediment-based reconstruction of Caribbean effective precipitation during the ‘Little ice age’ from freshwater pond, barbuda. *Holocene* 26, 1237–1247.
- Caffrey, M.A., Horn, S.P., Orvis, K.H., Haberyan, K.A., 2015. Holocene environmental change Laguna Saladilla, coastal north Hispaniola. *Palaeogeography, Palaeoclimatology, Palaeoecology* 4346, 9–22.
- Cant, R.V., Weech, P.S., 1986. A review of the factors affecting the development of Ghyben-Hertzberg lenses in the Bahamas. *J. Hydrol.* 84, 333–343.
- Carrillo-Bastos, A., Islebe, G.A., Torrescano-Valle, N., Gonzalez, N.E., 2010. Holocene vegetation and climate history of central Quintana Roo, Yucatan Peninsula, Mexico. *Review of Paleobotany and Palynology* 160, 189–196.
- Coutino, A., Stastna, M., Kovacs, S.E., Reinhardt, E., 2017. Hurricanes Ingrid and Manuel (2013) and their impact on the salinity of the meteoric water mass, quintana roo, Mexico. *J. Hydrol.* 551, 715–729.
- Crotty, K.J., 1982. Paleoenvironmental Interpretation of Ostracod Assemblages from Watlings Blue Hole, San Salvador Island, Bahamas. University of Akron, Akron, Ohio, p. 79.
- Crotty, K.J., Teeter, J.W., 1984. Post pleistocene salinity variations in a blue hole, San Salvador Island, Bahamas as interpreted from ostracode fauna. In: Teeter, J. (Ed.), *Proceedings of the 2nd Symposium on the Geology of the Bahamas, San Salvador Island, the Bahamas*, pp. 3–16.
- Daday, v.E., 1905. Untersuchungen über die Süßwasser-Mikrofauna Paraguays. *Abhandlungen aus dem Gesamtgebiete der Zoologie* 18, 1–374.
- Davis, R.E., Hayden, B.P., Gay, D.A., Phillips, W.L., Jones, G.V., 1997. The North Atlantic tropical anticyclone 10, 728–744.
- Dean Jr., W.E., 1974. Determination of carbonate and organic matter in calcareous sediments and sedimentary rocks by loss on ignition: comparison with other methods. *J. Sediment. Res.* 44.
- Deevey, E.S., Deevey, G.B., Brenner, M., 1980. Structure of zooplankton communities in the Peten Lake district Guatemala. In: Kerfoot, W.C. (Ed.), *The Evolution and Ecology of Zooplankton Communities*. University Press of New England, Hannover, New Hampshire, pp. 669–678.
- deMenocal, P., Ortiz, J., Guilderson, T., Sarnthein, M., 2000. Coherent high- and low-latitude climate variability during the Holocene Warm Period. *Science* 288, 2198–2202.
- Dix, G.R., Patterson, R.T., Park, L.E., 1999. Marine saline ponds as sedimentary archives of late Holocene climate and sea-level variation along a carbonate platform margin: Lee Stocking Island, Bahamas. *Palaeogeogr. Palaeoclimatol. Palaeoecol.* 150, 223–246.
- Donnelly, J.P., Woodruff, J.D., 2007. Intense hurricane activity over the past 5,000 years controlled by El Niño and the west african monsoon. *Nature* 447, 465–468.
- Dwyer, G.S., Teeter, J.W., 1991. Salinity history of a coastal salina, West Caicos, British West Indies. In: Bain, R.J. (Ed.), *Proceedings of the Fifth Symposium on the Geology of the Bahamas, Bahamian Field Station, San Salvador, The Bahamas*, pp. 65–73.
- Enfield, D.B., Alfaro, E., 1999. The dependence of Caribbean rainfall on the interaction of the tropical Atlantic and Pacific Oceans. *J. Clim.* 12, 2093–2103.
- Fensterer, C., Scholz, D., Hoffman, D.L., Spotl, C., Schroder-Ritzrau, A., Horn, C., Pajon, J.M., Mangini, A., 2013. Millennial-scale climate variability during the last 12.5 ka recorded in a Caribbean speleothem. *Earth Planet Sci. Lett.* 361, 143–151.
- France, R.L., 1995. Carbon-13 enrichment in benthic compared to planktonic algae: foodweb implications. *Mar. Ecol. Prog. Ser.* 124, 307–312.
- Fritz, S.C., Bjork, S., Rigsby, C.A., Baker, P.A., Calder-Church, A., Conley, D.J., 2011. Caribbean hydrological variability during the Holocene as reconstructed from crater lakes on the island of Grenada. *J. Quat. Sci.* 26, 829–838.
- Furtos, N.C., 1933. The Ostracoda of Ohio. *Bull. Ohio Biol. Surv.* 29.
- Furtos, N.C., 1936. Fresh-water ostracoda from Florida and North Carolina. *Am. Midl. Nat.* 17, 491–522.
- Gamble, D.W., Curtis, S., 2008. Caribbean precipitation: a review, model and prospect. *Prog. Phys. Geogr.* 32, 265–276.
- Gamble, D.W., Parnell, D.B., Curtis, S., 2008. Spatial variability of the Caribbean mid-summer drought and relation to the north Atlantic high circulation. *International Journal of Climate* 28, 343–350.
- Garcia-Pichel, F., Al-Horani, A.F., Farmer, J.D., Ludwig, R., Wade, B.D., 2004. Balance between microbial calcification and metazoan bioerosion in modern stromatolitic oncolites. *Geobiology* 2, 49–57.
- Gasse, F., 2000. Hydrological changes in the african tropics since the last glacial maximum. *Quat. Sci. Rev.* 19, 189–211.
- Giannini, A., Kushnir, Y., Cane, M.A., 2000. Interannual variability of caribbean rainfall, ENSO, and the Atlantic Ocean. *J. Clim.* 13, 297–311.
- Gischler, E., Gibson, M.A., Oschmann, W., 2008. Giant Holocene freshwater microbialites, Laguna Bacalar, quintana roo, Mexico. *Sedimentology* 55, 1293–1309.
- Glaser, P.H., Hansen, B.C.S., Donovan, J.J., Givnish, T.J., Stricker, C.A., Volin, J.C., 2012. Holocene dynamics of the Florida Everglades with respect to climate, dustfall, and tropical storms. *Proc. Natl. Acad. Sci. Unit. States Am.* 110, 17211–17216.
- Glunk, C., Dupraz, C., Braissant, O., Gallagher, K.L., Verrecchia, E.P., Visscher, P.T., 2011. Microbially mediated carbonate precipitation in a hypersaline lake, Big Pond (Eleuthera, Bahamas). *Sedimentology* 58.
- Gregory, B.R.B., Peros, M., Reinhardt, E.G., Donnelly, J.P., 2015. Middle-late Holocene Caribbean aridity inferred from foraminifera and elemental data in sediment

- cores from two Cuban lagoons. *Palaeogeogr. Palaeoclimatol. Palaeoecol.* 426, 229–241.
- Hastenrath, S., 1976. Variations in low-latitude circulation and extreme climatic events in the tropical Americas. *J. Atmos. Sci.* 33.
- Hastenrath, S., 1984. Interannual variability and annual cycle: mechanisms of circulation and climate in the tropical Atlantic Sector. *Mon. Weather Rev.* 112, 1097–1107.
- Hatcher, P.G., Simoneit, B.R.T., McKenzie, F.T., Neumann, A.C., Thorstenson, D.C., Gerchakov, S.M., 1982. Organic geochemistry and pore water chemistry of sediments from Mangrove Lake, Bermuda. *Org. Geochem.* 4, 93–112.
- Hatcher, P.G., Spiker, E.C., Szezerenyi, N.M., Maciel, G.E., 1984. Selective preservation and origin of petroleum-forming aquatic kerogen. *Nature* 305, 498–501.
- Haug, G.H., Hughen, K.A., Sigman, D.M., Peterson, L.C., Röhl, U., 2001. Southward migration of the intertropical convergence zone through the Holocene. *Science* 293, 1304–1308.
- Heiri, O., Lotter, A.F., Lemcke, G., 2001. Loss on ignition as a method for estimating organic and carbonate content in sediments: reproducibility and comparability of results. *J. Paleolimnol.* 25, 101–110.
- Herrera, E., Magaña, V., Caetano, E., 2015. Air–sea interactions and dynamical processes associated with the midsummer drought. *Int. J. Climatol.* 35, 1569–1578.
- Higuera-Gundy, A., Brenner, M., Hodell, D.A., Curtis, J.H., Leyden, B.W., Binford, M.W., 1999. A 10,300 ¹⁴C yr record of climate and vegetation change from Haiti. *Quat. Res.* 52, 159–170.
- Hodell, D.A., Brenner, M., Curtis, J.H., 2005a. Terminal Classic drought in the northern Maya lowlands inferred from multiple sediment cores in Lake Chichancanab (Mexico). *Quat. Sci. Rev.* 24, 1413–1427.
- Hodell, D.A., Brenner, M., Curtis, J.H., Gonzalez-Medina, R., CAn, E.I.-C., Guilderson, T.P., 2005b. Climate change on the Yucatan Peninsula during the Little Ice age. *Quat. Res.* 63, 109–121.
- Hodell, D.A., Brenner, M., Curtis, J.H., Guilderson, T., 2001. Solar forcing of drought frequency in the Maya Lowlands. *Science* 292, 1367–1370.
- Hodell, D.A., Curtis, J.H., Brenner, M., 1995. Possible role of climate in the collapse of Classic Maya civilization. *Nature* 375, 391–394.
- Hodell, D.A., Curtis, J.H., Jones, G.A., Higuera-Gundy, A., Brenner, M., Binford, M.W., Dorsey, K.T., 1991. Reconstruction of Caribbean climate change over the past 10,500 years. *Nature* 352, 790–793.
- Holding, S., Allen, D.M., 2015. From days to decades: numerical modeling of freshwater response to climate change stressor on small low-lying islands. *Hydrol. Earth Syst. Sci.* 19, 933–949.
- Holmes, J.A., 1997. Recent non-marine ostracoda from Jamaica, west Indies. *J. Micropalaeontol.* 16, 137–143.
- Holmes, J.A., 1998. A late Quaternary ostracod record from Wallywash Great Pond, a Jamaican marl lake. *J. Paleolimnol.* 19, 115–128.
- Hu, Y., Li, D., Liu, J., 2007. Abrupt seasonal variation of the ITCZ and the Hadley circulation. *Geophys. Res. Lett.* 34, L18814.
- Jury, M., Malmgren, B.A., Winter, A., 2007. Subregional precipitation climate of the Caribbean and relationships with ENSO and NAO. *J. Geophys. Res.* 112, 11.
- Jury, M.R., 2009. A quasi-decadal cycle in Caribbean climate. *J. Geophys. Res.: Atmosphere* 114, 8.
- Kennedy, L.M., Horn, S.P., Orvis, K.H., 2006. A 4000-year record of fire and forest history from Valle de Bao, Cordillera Central, Dominican Republic. *Palaeogeogr. Palaeoclimatol. Palaeoecol.* 231, 279–290.
- Keyser, D., 1975. Ostracoden aus den mangrovegebieten von Südwest-Florida. *Abhandlungen und Verhandlungen des Naturwissenschaftlichen Vereins in Hamburg* 18/19, 255–290.
- Keyser, D., 1977. Ecology of zoogeography of recent brackish-water ostracods (Crustacea) from south-west Florida. In: Löffler, H., Danielopol, D. (Eds.), *Aspects of the Ecology and Zoogeography of Recent and Fossil Ostracoda*. Dr. W. Junk Publishers, The Hague, pp. 207–222.
- Keyser, D., Schöning, C., 2000. Holocene ostracoda (Crustacea) from Bermuda. *Senckenberg. Lethaea* 80, 567–591.
- Khan, N.S., Ashe, E., Horton, B.P., Dutton, A., Kopp, R.E., Brocard, G., Engelhart, S.E., Hill, D.F., Peltier, W.R., Vane, C.H., Scatena, F.N., 2017. Drivers of Holocene sea-level change in the Caribbean. *Quat. Sci. Rev.* 155, 13–36.
- Kjellmark, E., 1996. Late Holocene climate change and human disturbance on Andros Island, Bahamas. *J. Paleolimnol.* 15, 133–145.
- Kovacs, S.E., Reinhardt, E.G., Stastna, M., Coutino, A., Werner, C., Collins, S.V., Devos, F., Le Mailliot, C., 2017. Hurricane Ingrid and tropical storm Hanna's effects on the salinity of the coastal aquifer, Quintana Roo, Mexico. *J. Hydrol.* 551, 732–714.
- Krutak, P.R., 1971. The recent ostracoda of Laguna Mandinga, Veracruz, Mexico. *Micropaleontology* 1–30.
- Lamb, A.L., Wilson, G.P., Leng, M.J., 2006. A review of coastal paleoclimate and relative sea-level reconstructions using $\delta^{13}C$ and C/N ratios in organic material. *Earth Sci. Rev.* 75, 29–57.
- Lane, C.S., Horn, S.P., Kerr, M.T., 2014. Beyond the Mayan Lowlands: impacts of the terminal classic drought in the Caribbean Antilles. *Quat. Sci. Rev.* 86, 89–98.
- Lane, C.S., Horn, S.P., Mora, C.I., Orvis, K.H., 2009. Late-Holocene paleoenvironmental change at mid-elevation on the Caribbean slope of the Cordillera Central, Dominican Republic: a multi-site, multi-proxy analysis. *Quat. Sci. Rev.* 28, 2239–2260.
- Legandre, P., Legendre, L., 1998. *Numerical Ecology*. Elsevier, Amsterdam.
- Leyden, B.W., Brenner, M., Dahlén, B.H., 1998. Cultural and climatic history of Coba, a lowland Maya city in Quintana Roo, Mexico. *Quat. Res.* 49, 833–839.
- Li, L., Li, W., Kushnir, Y., 2012a. Variation of the North Atlantic subtropical high western ridge and its implication to Southeastern US summer precipitation. *Clim. Dynam.* 39.
- Li, W., Li, L., Fu, R., Deng, Y., Wang, H., 2011. Changes to the north Atlantic subtropical high and its role in the intensification of summer rainfall variability in the southeastern United States. *J. Clim.* 24, 1499–1506.
- Li, W., Li, L., Ting, M., Liu, Y., 2012b. Intensification of Northern Hemisphere subtropical highs in a warming climate. *Nat. Geosci.* 5, 830–834.
- Magaña, V., Amdor, J.A., Medina, S., 1999. The midsummer drought over Mexico and Central America. *J. Clim.* 12, 1577–1588.
- Magaña, V., Caetano, E., 2005. Temporal evolution of summer convective activity over the Americas warm pools. *Geophys. Res. Lett.* 32, L02803.
- Malaizé, B., Bertran, P., Carbonel, P., Bonnissent, D., Charlier, K., Galop, D., Lambert, D., Serrand, N., Stouvenot, C., Pujol, C., 2011. Hurricanes in the Caribbean during the past 3700 years BP. *Holocene* 21, 911–924.
- Mangini, A., Blumbach, P., Verdes, P., Spotl, C., Scholz, D., Machel, H., Mahon, S., 2007. Combined records from a stalagmite from Barbados and from lake sediments in Haiti reveal variable seasonality in the Caribbean between 6.7 and 3 ka BP. *Quat. Sci. Rev.* 26, 1332–1342.
- Martin, E.R., Schumacher, C., 2011a. The Caribbean Low-level jet and its relationships with precipitation in IPCC AR4 Models. *American Meteorological Society* 24, 5935–5950.
- Martin, E.R., Schumacher, C., 2011b. Modulation of Caribbean precipitation by the Madden-Julian oscillation. *J. Clim.* 24, 813–824.
- Martin, P.H., Fahey, T.J., 2014. Mesoclimatic patterns shape the striking vegetation mosaic in the Cordillera Central, Dominican Republic. *Arctic Antarct. Alpine Res.* 46, 755–765.
- McGee, D., Donohoe, A., Marshall, J., Ferreira, D., 2014. Changes in ITCZ location and cross-equatorial heat transport at the last glacial maximum, Heinrich stadial 1, and the mid-Holocene. *Earth Planet Sci. Lett.* 390, 69–79.
- McLean, N.M., Stephenson, T.S., Taylor, M.A., Campbell, J.D., 2015. Characterization of future Caribbean rainfall and temperature extremes across rainfall zones. *Advances in Meteorology* 18.
- Medina-Elizalde, M., Burns, S.J., Lea, D.W., Asmerom, Y., von Gunten, L., Polyak, V., Vuille, M., Karmalkara, A., 2010. High resolution stalagmite climate record from the Yucatán Peninsula spanning the Maya terminal classic period. *Earth Planet Sci. Lett.* 298, 255–262.
- Méhes, G., 1914. Süßwasser-Ostracoden aus Columbian und Argentinien. *Mémoires de la Société naturelle de Neuchâtel* 5, 639–663.
- Meyer, J., Wrożyna, C., Gross, M., Leis, A., Piller, W.E., 2017. Morphological and geochemical variations of *Cyprideis* (Ostracoda) from modern waters of the northern tropics. *Limnology* 18, 251–273.
- Milne, G.A., Peros, M., 2013. Data-model comparison of Holocene sea-level change in the circum-Caribbean region. *Global Planet. Change* 107, 119–131.
- Morgan, G.S., Woods, C.A., 1986. Extinction and the zoogeography of West Indian land mammals. *Biol. J. Linn. Soc.* 28, 167–203.
- Moy, C.M., Seltzer, G.O., Rodbell, D.T., Anderson, D.M., 2002. Variability of El Niño/Southern Oscillation activity at millennial timescales during the Holocene. *Nature* 420, 162–165.
- Mullins, H.T., Lynts, G.W., 1977. Origin of the northwestern Bahama platform: review and interpretation. *Geol. Soc. Am. Bull.* 88, 1447–1461.
- Mylroie, J.E., Carew, J.L., 1995. Geology and karst geomorphology on San Salvador Island, Bahamas. *Carbonates Evaporites* 10, 193–206.
- Mylroie, J.E., Carew, J.L., Moore, A.L., 1995a. Blue holes: definitions and genesis. *Carbonates Evaporites* 10, 225–233.
- Mylroie, J.E., Carew, J.L., Vacher, H.L., 1995b. Karst development in the Bahamas and Bermuda. In: Curran, H.A., White, B. (Eds.), *Terrestrial and Shallow Marine Geology of the Bahamas and Bermuda*. Geologic Society of America, pp. 251–267.
- Neumann, A.C., Land, L.S., 1975. Lime mud deposition and calcareous algae in the Bight of Abaco, Bahamas. *J. Sediment. Petrol.* 45, 763–786.
- Nyberg, J., Malmgren, B.A., Winter, A., Jury, M.R., Kilbourne, K.H., Quinn, T.M., 2007. Low Atlantic hurricane activity in the 1970s and 1980s compared to the past 270 years. *Nature* 477, 698–701.
- Oppo, D.W., McManus, J.F., Cullen, J.L., 2003. Deep water variability in the Holocene epoch. *Nature* 422, 277–278.
- Park Bousch, L.E., Myrbo, A., Michelson, A., 2014. A qualitative and quantitative model for climate-driven lake formation on carbonate platforms based on examples from the Bahamian archipelago. *Carbonates Evaporites* 29, 409–418.
- Patterson, R.T., Fishbein, E., 1989. Re-examination of the statistical methods used to determine the number of point counts needed for micropaleontological quantitative research. *J. Paleontol.* 63, 245–248.
- Pérez, L., Lorenschat, J., Brenner, M., Scharf, B., Schwalb, A., 2010a. Extant freshwater ostracodes (Crustacea: ostracoda) from Lago Peten Itza, Guatemala. *Rev. Biol. Trop.* 58, 871–895.
- Pérez, L., Lorenschat, J., Bugja, R., Brenner, M., Scharf, B.S., Schwalb, A., 2010b. Distribution, diversity and ecology of modern freshwater ostracodes (Crustacea), and hydrochemical characteristics of Lago Peten Itza, Guatemala. *J. Limnol.* 69, 146–159.
- Peros, M., Gregory, B., Mateos, F., Reinhardt, E., Desloges, J., 2015. Late Holocene record of lagoon evolution, climate change, and hurricane activity from southeastern Cuba. *Holocene* 1–15.
- Peterson, L.C., Overpeck, J.T., Kipp, N.G., Imbrie, J., 1991. A high-resolution Late Quaternary upwelling record from the anoxic Carico Basin, Venezuela. *Paleoceanography* 6, 99–119.

- Pilsbry, H.A., 1934. Review of the Planorbidae of Florida, with notes on other members of the family. *Proc. Acad. Nat. Sci. Phila.* 86, 29–66.
- Rasmussen, K.A., Haddad, R.I., Neuman, A.C., 1990. Stable-isotope record of organic carbon from an evolving carbonate banktop, Bight of Abaco, Bahamas. *Geology* 18, 790–794.
- Rasmussen, K.A., Neumann, A.C., 1988. Holocene overprints of pleistocene paleokarst: Bight of Abaco, Bahamas. In: James, N.P., Choquette, P.W. (Eds.), *Paleokarst*. Springer-Verlag, New York, pp. 132–148.
- Reimer, P.J., Bard, E., Bayliss, A., Beck, J.W., Blackwell, P.G., Bronk Ramsey, C., Buck, C.E., Cheng, H., Edwards, R.L., Friedrich, M., Grootes, P.M., Guilderson, T.P., Hafliðason, H., Hájdas, I., Hatte, C., Heaton, T.J., Hoffman, D.L., Hogg, A.G., Hughen, K.A., Kaiser, K.F., Kromer, B., Manning, S.W., Niu, M., Reimer, R.W., Richards, D.A., Scott, E.M., Southon, J.R., Stafford, R.A., Turney, C.S.M., van der Plicht, J., 2013. IntCal13 and Marine13 radiocarbon age calibration curves 0–50,000 years Cal BP. *Radiocarbon* 55, 1869–1887.
- Schmitter-Soto, J.J., Comín, F.A., Escobar-Briones, E., Herrera-Silveira, J., Alcocer, J., Suárez-Morales, E., Elías-Gutiérrez, M., Díaz-Arce, V., Marín, L.E., Steinich, B., 2002. Hydrogeochemical and biological characteristics of cenotes in the Yucatan Peninsula (SE Mexico). *Hydrobiologia* 467, 215–228.
- Schneider, T., Bischoff, T., Haug, G.H., 2014. Migrations and dynamics of the inter-tropical convergence zone. *Nature* 513, 46–53.
- Schnurrenberger, D., Russell, J., Kelts, K., 2003. Classification of lacustrine sediments based on sedimentary components. *J. Paleolimnol.* 29, 141–154.
- Sharpe, R.W., 1908. A further report on the Ostracoda of the United States. *Proc. U. S. Natl. Mus* 35, 399–430.
- Sipahioglu, S.M., Park, L.E., Siewers, F.D., 2010. In: Siewers, F.D., Martin, J.B. (Eds.), *Proceedings of the 14th Symposium of the Geology of the Bahamas and other Carbonate Regions*. Gerace Research Center, San Salvador Island, The Bahamas, pp. 220–236.
- Slayton, I., 2010. A Vegetation History from Emerald Pond, Great Abaco Island, the Bahamas, Based on Pollen Analysis. MSc Thesis. University of Tennessee, Knoxville, p. 85.
- Soto-Centeno, J.A., Steadman, D.W., 2015. Fossils reject climate change as the cause of extinction in Caribbean bats. *Sci. Rep.* 5.
- Soulié-Marsche, I., 2008. Charophytes, indicators for low salinity phases in North African sebkhet. *J. Afr. Earth Sci.* 51, 69–76.
- Soulié-Marsche, I., Garcia, A., 2015. Gyrogonites and oospores, complementary viewpoints to improve the study of the charophytes (Charales). *Aquat. Bot.* 120, 7–17.
- Steadman, D.W., Franz, R., Morgan, G.S., Albury, N.A., Kakuk, B., Broad, K., Franz, S.E., Tinker, K., Pateman, M.P., Lott, T.A., Jarzen, D.M., Dilcher, D.L., 2007. Exceptionally well preserved late Quaternary plant and vertebrate fossils from a blue hole on Abaco, the Bahamas. *Proc. Natl. Acad. Sci. Unit. States Am.* 104, 19897–19902.
- Swain, F.M., 1955. Ostracoda of San Antonio Bay, Texas. *J. Paleontol.* 29, 561–646.
- Teeter, J., 1980. Ostracoda of the lake flirt formation (pleistocene) of southern Florida. *Micropaleontology* 337–355.
- Teeter, J.W., 1989. Holocene salinity history of the saline lakes of San Salvador Island, Bahamas. In: Curran, H.A., Bain, R.J., Carew, J.L., Mylroie, J., Teeter, J.W., White, B. (Eds.), *Pleistocene and Holocene Carbonate Environments on San Salvador Island, Bahamas, San Salvador, the Bahamas*, pp. 35–39.
- Teeter, J.W., 1995a. Holocene saline lake history, San Salvador Island, Bahamas. *Spec. Pap. Geol. Soc. Am.* 117–124.
- Teeter, J.W., 1995b. Holocene saline lake history, San Salvador Island, Bahamas. In: Curan, H.A., White, B. (Eds.), *Terrestrial and Shallow Marine Geology of the Bahamas and Bermuda*, pp. 117–124.
- Teeter, J.W., Quick, T.J., 1990. Magnesium-salinity relation in the saline lake ostracode *Cyprideis americana*. *Geology* 18, 220–222.
- Torrescano-Valle, N.A., Islebe, G.A., 2015. Holocene paleoecology, climate history and human influence in the southwestern Yucatan Peninsula. *Review of Paleobotany and Palynology* 217, 1–8.
- van Hengstum, P.J., Bernhard, J.M., 2016. A new species of benthic foraminifera from an inland Bahamian carbonate marsh. *J. Foraminif. Res.* 46, 193–2000.
- van Hengstum, P.J., Donnelly, J.P., Fall, P.L., Toomey, M.R., Albury, N.A., Kakuk, B., 2016. The intertropical convergence zone modulates intense hurricane strikes on the western North Atlantic margin. *Sci. Rep.* 6, 21728.
- van Hengstum, P.J., Reinhardt, E.G., Beddows, P.A., Gabriel, J.J., 2010. Investigating linkages between Holocene paleoclimate and paleohydrogeology preserved in a Yucatan underwater cave. *Quat. Sci. Rev.* 29, 2788–2798.
- van Hengstum, P.J., Reinhardt, E.G., Beddows, P.A., Huang, R.J., Gabriel, J.J., 2008. Thecamoebians (testate amoebae) and foraminifera from three anchialine cenotes in Mexico: low salinity (1.5–4.5 psu) faunal transitions. *J. Foraminif. Res.* 38, 305–317.
- van Hengstum, P.J., Scott, D.B., 2011. Ecology of foraminifera and habitat variability in an underwater cave: distinguishing anchialine versus submarine cave environments. *J. Foraminif. Res.* 41, 201–229.
- van Hengstum, P.J., Scott, D.B., 2012. Sea-level rise and coastal circulation controlled Holocene groundwater development and caused a meteoric lens to collapse 1600 years ago in Bermuda. *Marine Micropaleontology* 90–91, 29–43.
- van Hengstum, P.J., Scott, D.B., Gröcke, D.R., Charette, M.A., 2011. Sea level controls sedimentation and environments in coastal caves and sinkholes. *Mar. Geol.* 286, 35–50.
- Van Morkhoven, F.P.C.M., 1963. *Post-palaeozoic Ostracoda: Their Morphology, Taxonomy, and Exonomic Use, Volume 2: Generic Descriptions*. Elsevier Publishing Company, Amsterdam.
- Wahl, D., Byrne, R., Anderson, L., 2014. An 8700 year paleoclimate reconstruction from the southern Maya lowlands. *Quat. Sci. Rev.* 103, 19–25.
- Waldeab, S., Schneider, R.R., Kölling, M., Wefer, G., 2005. Holocene African droughts relate to eastern equatorial cooling. *Geology* 33, 981–984.
- Wang, C., 2007. Variability of the Caribbean low-level jet and its relations to climate. *Clim. Dynam.* 29, 411–422.
- Wang, C., Enfield, D.B., Lee, S.-K., Landsea, C.W., 2006. Influences of the Atlantic warm pool on western hemisphere summer rainfall and atlantic hurricanes. *J. Clim.* 3011–3028.
- Watts, W.A., Hansen, B.C.S., 1986. Holocene climate and vegetation of Bermuda. *Pollen Spores* 28, 355–364.
- Whitaker, F.F., Smart, P.L., 1997. Hydrogeology of the Bahamian archipelago. In: Vacher, H.L., Quinn, T.M. (Eds.), *Geology and Hydrogeology of Carbonate Islands*. Elsevier, Amsterdam, pp. 183–216.
- Whyte, F.S., Taylor, M.A., Stephenson, T.S., Campbell, J.D., 2008. Features of the Caribbean low level jet. *Int. J. Climatol.* 28, 119–128.
- Winter, A., Miller, T., Kushnir, Y., Sinha, A., Timmermann, A., Jury, M.R., Gallup, C., Cheng, H., Edwards, R.L., 2011. Evidence for 800 years of North atlantic multi-decadal variability from a Puerto Rican speleothem. *Earth Planet Sci. Lett.* 308, 23–28.
- Wooller, M.J., Behling, H., Guerrero, J.L., Jantz, N., Zweigert, M.E., 2009. Late Holocene hydrologic and vegetation changes at Turneffe Atoll, Belize, compared with records from mainland Central America and Mexico. *Palaos* 24, 650–656.